J|A|C|S ARTICLES

Published on Web 08/05/2010

Fluxionality of $[(Ph_3P)_3M(X)]$ (M = Rh, Ir). The Red and Orange Forms of $[(Ph_3P)_3Ir(Cl)]$. Which Phosphine Dissociates Faster from Wilkinson's Catalyst?

Jenni Goodman,[‡] Vladimir V. Grushin,*[,†,§] Roman B. Larichev,[†] Stuart A. Macgregor,*[,‡] William J. Marshall,[†] and D. Christopher Roe*[,†]

Central Research & Development, E. I. DuPont de Nemours & Co., Inc., Experimental Station, Wilmington, Delaware 19880, School of Engineering and Physical Sciences, William H. Perkin Building, Heriot-Watt University, Edinburgh EH14 4AS, U.K., and The Institute of Chemical Research of Catalonia (ICIQ), Tarragona 43007, Spain

Received May 10, 2010; E-mail: vgrushin@iciq.es; s.a.macgregor@hw.ac.uk; chris.roe@usa.dupont.com

Abstract: NMR studies of intramolecular exchange in $[(Ph_3P)_3Rh(X)]$ (X = CF_3, CH_3, H, Ph, Cl) have produced full sets of activation parameters for X = CH_3 ($E_a = 16.4 \pm 0.6$ kcal mol^{-1}, $\Delta H^{\ddagger} = 16.0 \pm 0.6$ kcal mol^{-1}, and $\Delta S^{\ddagger} = 12.7 \pm 2.5$ eu), H ($E_a = 10.7 \pm 0.2$ kcal mol^{-1}, $\Delta H^{\ddagger} = 10.3 \pm 0.2$ kcal mol^{-1}, and $\Delta S^{\ddagger} = -7.2 \pm 0.8$ eu), and Cl ($E_a = 16.3 \pm 0.2$ kcal mol^{-1}, $\Delta H^{\ddagger} = 15.7 \pm 0.2$ kcal mol^{-1}, and $\Delta S^{\ddagger} = -0.8 \pm 0.8$ eu). Computational studies have shown that for strong trans influence ligands (X = H, Me, Ph, CF_3), the rearrangement occurs via a near-trigonal transition state that is made more accessible by bulkier ligands and strongly donating X. The exceedingly fast exchange in novel $[(Ph_3P)_3Rh(CF_3)]$ (12.1 s^{-1} at -100 °C) is due to strong electron donation from the CF_3 ligand to Rh, as demonstrated by computed charge distributions. For weaker donors X, this transition state is insufficiently stabilized, and hence intramolecular exchange in $[(Ph_3P)_3Rh(Cl)]$ proceeds via a different, spin-crossover mechanism involving triplet, distorted-tetrahedral $[(Ph_3P)_3Rh(Cl)]$ as an intermediate. Simultaneous intermolecular exchange of $[(Ph_3P)_3Rh(Cl)]$ with free PPh_3 (THF) via a dissociative mechanism occurs exclusively from the sites cis to Cl ($E_a = 19.0 \pm 0.3$ kcal mol^{-1}, $\Delta H^{\ddagger} = 18.5 \pm 0.3$ kcal mol^{-1}, and $\Delta S^{\ddagger} = 4.4 \pm 0.9$ eu). Similar exchange processes are much slower for $[(Ph_3P)_3Ir(Cl)]$ which has been found to exist in orange and red crystallographic forms isostructural with those of $[(Ph_3P)_3Rh(Cl)]$.

Introduction

Complexes of the type $[(R_3P)_3M(X)]$ (M = Rh, Ir; X = anionic ligand) are ubiquitous in chemistry. For instance, Wilkinson's catalyst, $[(Ph_3P)_3Rh(Cl)]$ (**1**),[1,2] is one of the most important compounds in organometallic synthesis and catalysis, and its iridium congener, $[(Ph_3P)_3Ir(Cl)]$ (**2**), is also widely used and has been known for nearly as long.[3] Understanding the structural properties and solution behavior of $[(R_3P)_3M(X)]$ is of the essence to both fundamental science and the development of new applications for this class of compounds. Surprisingly, however, after 45 years of extensive studies of **1** and **2**, some critical basic information is still missing on both complexes. For instance, it has been widely known[4] since the original 1973 Halpern−Wong report[4a] that PPh_3 dissociation from **1** produces $[(Ph_3P)_2Rh(Cl)]$, the key 3-coordinate species that is orders of magnitude more reactive toward H_2 in olefin hydrogenation[1c] and crucial for many other stoichiometric and catalytic reactions employing **1**.[2] However, despite the recognized importance of PPh_3 loss from **1**, it is still unknown *which* phosphine (trans or cis to Cl) dissociates faster. Furthermore, while **1** has long been established to exist in two structurally characterized polymorphic forms, red and orange,[5] there have been no reports of a single-crystal X-ray diffraction study of **2**.[6,7]

Of particular interest is the phenomenon of fluxionality of $[(R_3P)_3M(X)]$. Numerous structural studies (see below) have indicated that in the solid state all such species exhibit distorted square-planar geometries. However, as early as 1967−1968, Keim reported that $[(Ph_3P)_3Rh(X)]$ (X = Me, H)[8,9] displayed equivalency of all three PPh_3 ligands in solution. Independently

[†] DuPont CR&D.
[‡] Heriot-Watt University.
[§] ICIQ.

(1) (a) Young, J. F.; Osborne, J. A.; Jardine, F. H.; Wilkinson, G. *Chem. Commun.* **1965**, 131. (b) Bennett, M. A.; Longstaff, P. A. *Chem. Ind. (London)* **1965**, 846. (c) Osborn, J. A.; Jardine, F. H.; Young, J. F.; Wilkinson, G. *J. Chem. Soc. A* **1966**, 1711.
(2) For a review, see: Jardine, F. H. *Prog. Inorg. Chem.* **1981**, *28*, 63.
(3) (a) Bennett, M. A.; Milner, D. L. *Chem. Commun.* **1967**, 581. (b) Collman, J. P.; Kubota, M.; Vastine, F. D.; Sun, J. Y.; Kang, J. W. *J. Am. Chem. Soc.* **1968**, *90*, 5430. (c) Bennett, M. A.; Milner, D. L. *J. Am. Chem. Soc.* **1969**, *91*, 6983.
(4) (a) Halpern, J.; Wong, C. S. *J. Chem. Soc., Chem. Commun.* **1973**, 629. (b) Wink, D. A.; Ford, P. C. *J. Am. Chem. Soc.* **1987**, *109*, 436. (c) Duckett, S. B.; Newell, C. L.; Eisenberg, R. *J. Am. Chem. Soc.* **1994**, *116*, 10548.
(5) Bennett, M. J.; Donaldson, P. B. *Inorg. Chem.* **1977**, *16*, 655.
(6) By visual comparison of X-ray powder patterns, $[(Ph_3P)_3Ir(Cl)]$ has been found isomorphous with $[(Ph_3P)_3Rh(Br)]$ and the orange form of **1**.[3c]
(7) An X-ray structure of the cobalt counterpart, $[(Ph_3P)_3Co(Cl)]$, has been reported. As expected, $[(Ph_3P)_3Co(Cl)]$ is tetrahedral. See: Cassidy, J. M.; Whitmire, K. H. *Acta Crystallogr. C* **1991**, *C47*, 2094.
(8) Keim, W. *J. Organomet. Chem.* **1967**, *8*, P25; **1968**, *14*, 179.
(9) Dewhirst, K. C.; Keim, W.; Reilly, C. A. *Inorg. Chem.* **1968**, *7*, 546.

and simultaneously, Eaton and Suart[10] provided indications that **1** undergoes both intra- and intermolecular phosphine exchange in $CDCl_3$. Since then, similar observations of intramolecular phosphine rearrangement have been made for more $[(R_3P)_3Rh(X)]$ complexes, where X = H,[11] Cl,[12] Alk,[13] Ar,[14] and CF_3.[15,16] On the other hand, other members of the family (e.g., X = F,[14,17] OR,[18] NR_2,[19] and some others[20]) do not exhibit obvious signs of stereochemical nonrigidity at ambient temperature. Clearly, fluxionality of $[(R_3P)_3Rh(X)]$ strongly depends on the nature of the anionic ligand X. We have recently communicated[15] a preliminary investigation of the mechanism of intramolecular phosphine exchange in $[(Ph_3P)_3Rh(X)]$, where X is a strong trans influence ligand.

In this paper, we report a detailed experimental and computational study of mechanisms of fluxionality of a series of complexes $[(Ph_3P)_3M(X)]$ (M = Rh, Ir). This work indicates that depending on the nature of X, intramolecular phosphine exchange can be governed by different mechanisms. The first in the series was a novel, uniquely fluxional complex, $[(Ph_3P)_3Rh(CF_3)]$ (**3**), which maintains fast phosphine exchange at temperatures as low as −100 °C. This complex was key for clarification of the ligand exchange mechanism in $[(R_3P)_3Rh(X)]$ and a better understanding of the long-puzzling nature of bonding in perfluoroalkyl metal complexes. We also report herein our serendipitous finding of two polymorphic forms of $[(Ph_3P)_3Ir(Cl)]$, which are not only red and orange in color but also pairwise isostructural with those of Wilkinson's catalyst. In sharp contrast with the striking crystallographic similarities between $[(Ph_3P)_3Ir(Cl)]$ and $[(Ph_3P)_3Rh(Cl)]$, the two exhibit markedly different solution behavior. Finally, we answer the long-standing question of which phosphine in Wilkinson's catalyst dissociates from the metal faster to produce $[(Ph_3P)_2Rh(Cl)]$, a key active species in catalysis with **1**.

Experimental Studies

Fluxionality Criteria for $[(R_3P)_3M(X)]$ (M = Rh, Ir). The ultimate method to judge the stereochemical rigidity of such species in solution is ^{31}P NMR. Well-resolved A_2BX (Rh) and A_2B (Ir) ^{31}P NMR patterns with no unambiguous signs of exchange at ambient temperature are conventionally viewed as an indication of rigidity on the NMR time scale. This was also the benchmark that was employed in our preliminary work,[15] leading us to incautiously state that **1** is stereochemically rigid in solution at room temperature. Although certainly useful in the vast majority of instances where no dynamic NMR data are available, this criterion is rather crude. Indeed, while exhibiting a clear A_2BX ^{31}P NMR pattern with no obvious signs of exchange at room temperature, Wilkinson's catalyst (**1**) is nonetheless measurably fluxional, as has been shown by Brown, Evans, and Lucy[12] in a DANTE spin saturation transfer experiment. It is conceivable that all $[(Ph_3P)_3Rh(X)]$ are fluxional in solution, albeit to a different extent.

$[(Ph_3P)_3Rh(CF_3)]$ (3). This new complex was the starting point of the entire project. Our long-standing interest in organometallic fluorine chemistry[14,15,17,21] prompted us to attempt the synthesis of $[(Ph_3P)_3Rh(CF_3)]$, the trifluoromethyl analogue of Wilkinson's catalyst.[22] As briefly communicated in our preliminary report,[15] the reaction of $[(Ph_3P)_3Rh(F)]$[14,17] with Ruppert's reagent (CF_3SiMe_3) produced isolable *trans*-$[(Ph_3P)_2Rh(CF_2)(F)]$ (Figure 1), apparently via α-F-elimination from the intermediate $[(Ph_3P)_3Rh(CF_3)]$ (**3**) (eq 1).[23−25] Although evidence was obtained for the same composition of $[(Ph_3P)_2Rh(CF_2)(F)]$ in the solid state in bulk (see the Experimental Section), on dissolution in benzene, toluene, or THF the preisolated carbene complex quickly equilibrated with a number of species, including **3**. Indeed, the room-temperature ^{19}F NMR spectra of the

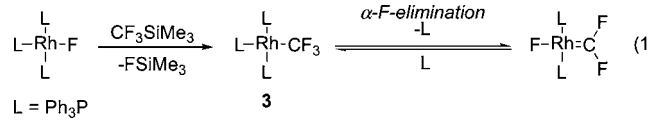

preisolated and recrystallized carbene complex displayed a doublet from Rh═CF_2 (2F) at 105.6 ppm in toluene-d_8 or 108.6 ppm (J_{F-Rh} = 33 Hz) in THF-d_8, along with a broad resonance at ca. −220 ppm from Rh−F (1F), and a sharp doublet of quartets from **3**. The F−Rh═CF_2 to Rh−CF_3 ratio was temperature dependent, with lower temperatures favoring the formation of **3**. The presence of the latter pointed to phosphine dissociation from $[(Ph_3P)_2Rh(CF_2)(F)]$, conceivably producing dinuclear complexes such as $[(Ph_3P)_2Rh_2(CF_2)_2(F)_2]$, congeners of the known[26] chloro carbonyl dimers $[(Ph_3P)_2Rh_2(CO)_2(Cl)_2]$. These observations accord with the ^{31}P NMR spectra of preisolated $[(Ph_3P)_2Rh(CF_2)(F)]$, which exhibited only the doublet of quartets from **3** at room temperature. At lower temperatures (0 to −60 °C), broad unresolved ^{31}P resonances appeared slightly upfield from the signal from **3**. However, addition of excess PPh_3 to this multicomponent solution efficiently shifted all equilibria to **3** as the only NMR-detectable

(10) Eaton, D. R.; Suart, S. R. *J. Am. Chem. Soc.* **1968**, *90*, 4170.
(11) Strauss, S. H.; Diamond, S. E.; Mares, F.; Shriver, D. F. *Inorg. Chem.* **1978**, *17*, 3064.
(12) Brown, J. M.; Evans, P. L.; Lucy, A. R. *J. Chem. Soc., Perkin Trans. 2* **1987**, 1589.
(13) Price, R. T.; Andersen, R. A.; Muetterties, E. L. *J. Organomet. Chem.* **1989**, *376*, 407.
(14) Macgregor, S. A.; Roe, D. C.; Marshall, W. J.; Bloch, K. M.; Bakhmutov, V. I.; Grushin, V. V. *J. Am. Chem. Soc.* **2005**, *127*, 15304.
(15) Goodman, J.; Grushin, V. V.; Larichev, R. B.; Macgregor, S. A.; Marshall, W. J.; Roe, D. C. *J. Am. Chem. Soc.* **2009**, *131*, 4236.
(16) Vicente, J.; Gil-Rubio, J.; Guerro-Leal, J.; Bautista, D. *Dalton Trans.* **2009**, 3854.
(17) Grushin, V. V.; Marshall, W. J. *J. Am. Chem. Soc.* **2004**, *126*, 3068.
(18) See, for example: (a) Kuznetsov, V. F.; Yap, G. P. A.; Bensimon, C.; Alper, H. *Inorg. Chim. Acta* **1998**, *280*, 172. (b) Osakada, K.; Ishii, H. *Inorg. Chim. Acta* **2004**, *357*, 3007. (c) Zhao, P.; Incarvito, C. D.; Hartwig, J. F. *J. Am. Chem. Soc.* **2006**, *128*, 3124.
(19) Zhao, P.; Krug, C.; Hartwig, J. F. *J. Am. Chem. Soc.* **2005**, *127*, 12066.
(20) Carlton, L. *Magn. Reson. Chem.* **2004**, *42*, 760.
(21) (a) Grushin, V. V. *Acc. Chem. Res.* **2010**, *43*, 160. (b) Macgregor, S. A. *Chem. Soc. Rev.* **2007**, *36*, 67. (c) Grushin, V. V. *Chem.—Eur. J.* **2002**, *8*, 1006.
(22) For reported CF_3−Rh complexes, see: (a) van der Boom, M. E.; Ben-David, Y.; Milstein, D. *Chem. Commun.* **1998**, 917. (b) van der Boom, M. E.; Ben-David, Y.; Milstein, D. *J. Am. Chem. Soc.* **1999**, *121*, 6652. (c) Vicente, J.; Gil-Rubio, J.; Bautista, D. *Inorg. Chem.* **2001**, *40*, 2636. (d) Vicente, J.; Gil-Rubio, J.; Guerrero-Leal, J.; Bautista, D. *Organometallics* **2004**, *23*, 4871. (e) Vicente, J.; Gil-Rubio, J.; Guerrero-Leal, J.; Bautista, D. *Organometallics* **2005**, *24*, 5634. (f) See also refs 15 and 16.
(23) Brothers, J. P.; Roper, W. R. *Chem. Rev.* **1988**, *88*, 1293.
(24) For more recent well-defined examples of F-α-elimination, see: (a) Huang, D.; Koren, P. R.; Folting, K.; Davidson, E. R.; Caulton, K. G. *J. Am. Chem. Soc.* **2000**, *122*, 8916. (b) Huang, D.; Caulton, K. G. *J. Am. Chem. Soc.* **1997**, *119*, 3185.
(25) The formation of both $[(Ph_3P)_2Rh(CF_2)(F)]$ and $[(Ph_3P)_3Rh(CF_3)]$ on treatment of $[(Ph_3P)_3RhCl]$ with $[M(CF_3)_2]$ (M = Cd, Hg) has been previously proposed but neither complex was detected due to facile hydrolysis leading to Rh carbonyl species: Burrell, A. K.; Clark, G. R.; Jeffrey, J. G.; Rickard, C. E. F.; Roper, W. R. *J. Organomet. Chem.* **1990**, *388*, 391.
(26) Rotondo, E.; Battaglia, G.; Giordano, G.; Cusmano, F. P. *J. Organomet. Chem.* **1993**, *450*, 245.

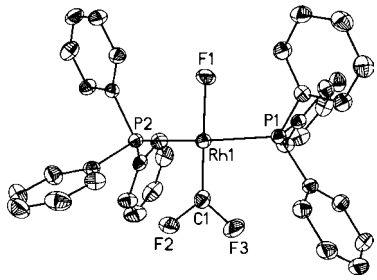

Figure 1. ORTEP drawing of [$(Ph_3P)_2Rh(CF_2)(F)$]. Selected bond distances (Å) and angles (deg): Rh−C 1.820(3); Rh−F(1) 1.994(2); Rh−P(2) 2.335(1); Rh−P(1) 2.349(1); C−Rh−F(1) 177.0(1); P(2)−Rh−P(1) 169.0(1); F(3)−C−F(2) 100.0(2); F(3)−C−Rh 130.8(2); F(2)−C−Rh 129.1(2).[15]

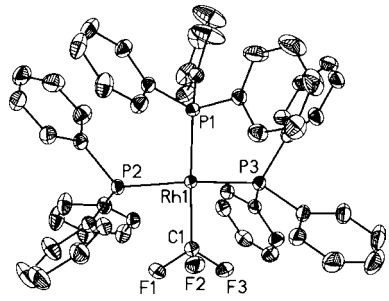

Figure 2. ORTEP drawing of [$(Ph_3P)_3Rh(CF_3)$] (**3**). Selected bond distances (Å) and angles (deg): Rh−C 2.096(2); Rh−P(2) 2.310(1); Rh−P(1) 2.313(1); Rh−P(3) 2.337(1); F(1)−C 1.376(2); F(2)−C 1.398(2); F(3)−C 1.380(2); C−Rh−P(1) 163.5(1); P(2)−Rh−P(3) 156.5(1); F(1)−C−F(3) 101.3(1); F(1)−C−F(2) 101.7(1); F(3)−C−F(2) 101.6(1).[15]

species. This allowed for high-yield (84%) isolation and full characterization of **3**, including X-ray analysis (Figure 2).

Sharp doublets of quartets in the ^{19}F and ^{31}P NMR spectra of [$(Ph_3P)_3Rh(CF_3)$] (with extra PPh_3 in THF-d_8) in the temperature range of 25 to −60 °C indicated fast *intramolecular* ligand exchange. Only at −100 °C was the exchange slow enough to observe two ^{31}P broad doublets at 33.5 ppm (2P, $J_{Rh-P} = 175$ Hz) and 30.5 ppm (1P, $J_{Rh-P} = 120$ Hz). At that temperature, magnetization transfer experiments allowed for exchange rate measurement of 12.1 s^{-1}. Activation parameters could not be determined because temperatures below −100 °C were not attainable.

[$(Ph_3P)_3Rh(H)$]. Shriver and co-workers[11] have reported a VT ^{31}P NMR study of [$(Ph_3P)_3Rh(H)$] to demonstrate its fluxionality and estimate a PPh_3 exchange rate of 230 s^{-1} at −13 °C. In our work, exchange rates for [$(Ph_3P)_3Rh(H)$] in THF-d_8 (24.9 ppm, 2P, dd, $J_{Rh-P} = 171$ Hz and 19.7 ppm,1P, dt, $J_{Rh-P} = 142$ Hz, $J_{P-P} = 25$ Hz at −70 °C) were measured in the temperature range of −30 to −70 °C (Table 1), which allowed for the determination of activation parameters: $E_a = 10.7 \pm 0.2$ kcal mol^{-1}, $\Delta G^{\ddagger} = 11.9$ kcal mol^{-1} (calculated at −50 °C), $\Delta H^{\ddagger} = 10.3 \pm 0.2$ kcal mol^{-1}, and $\Delta S^{\ddagger} = -7.2 \pm 0.8$ eu.

Table 1. Exchange Rates for [$(Ph_3P)_3Rh(H)$] in THF-d_8

temp, °C	k,[a] s^{-1}
−30	80.6 (3.24)
−40	30.3 (1.10)
−50	11.0 (0.37)
−60	3.4 (0.10)
−70	1.0 (0.04)

[a] Standard deviation in parentheses.

[$(Ph_3P)_3Rh(CH_3)$]. This complex was also studied by VT ^{31}P NMR. The coalescence temperature was around 20 °C, and a well-resolved first-order A_2BX spectrum (43.7 ppm, 2P, dd, $J_{Rh-P} = 172$ Hz and 34.7 ppm, 1P, dt, $J_{Rh-P} = 131$ Hz, $J_{P-P} = 30$ Hz at −50 °C) could be observed already at −10 °C. Measuring exchange rates in the temperature range of −10 to −50 °C (Table 2) allowed for the determination of activation parameters: $E_a = 16.4 \pm 0.6$ kcal mol^{-1}, $\Delta G^{\ddagger} = 12.9$ kcal mol^{-1} (calculated at −30 °C), $\Delta H^{\ddagger} = 16.0 \pm 0.6$ kcal mol^{-1}, and $\Delta S^{\ddagger} = 12.7 \pm 2.5$ eu.

Numerous attempts to determine an X-ray structure of [$(Ph_3P)_3Rh(CH_3)$] were only partially successful, probably because it is highly unstable toward cyclometalation. Eventually a structure was obtained, but its poor quality prevents us from publishing it in detail. The poor quality results from weak diffraction caused by the small crystallite size and complete disorder for seven of the nine phenyl groups. Nonetheless, some geometry parameters are trustworthy and hence will be used in the Discussion section.

Table 2. Exchange Rates for [$(Ph_3P)_3Rh(CH_3)$] in THF-d_8

temp, °C	k,[a] s^{-1}
−10	178.0 (4.57)
−20	52.8 (0.82)
−30	13.7 (0.18)
−40	3.40 (0.06)
−50	0.61 (0.02)

[a] Standard deviation in parentheses.

[$(Ph_3P)_3Rh(Ph)$]. We have previously reported[14] that the room-temperature ^{31}P NMR spectrum of this complex displayed an unsymmetrical doublet. As was found in this work, the doublet became symmetrical at 40 °C ($J_{P-Rh} = 163$ Hz). Below the coalescence point around −20 °C, a complex second-order spectrum was observed, indicating apparent stereochemical rigidity on the NMR time scale. Second-order ^{31}P NMR spectra have been previously reported for similar Rh(I) σ-aryls [$(Me_3P)_3Rh(Ar)$] (Ar = Ph, *m*-Tol, *p*-Tol).[13]

[$(Ph_3P)_3Rh(Cl)$] (Wilkinson's Catalyst). Brown's DANTE spin saturation transfer study[12] has kinetically quantified two phosphine exchange processes occurring in toluene−CH_2Cl_2 solutions of Wilkinson's catalyst, intramolecular (22 s^{-1} at 24 °C) and intermolecular (0.31 s^{-1} at 30 °C). In this work, we studied [$(Ph_3P)_3Rh(Cl)$] in THF-d_8 for consistency with the previously obtained results for other [$(Ph_3P)_3Rh(X)$]. Both intramolecular and intermolecular exchange processes were detected for [$(Ph_3P)_3Rh(Cl)$] by ^{31}P NMR magnetization transfer experiments in the temperature range of 0 to 50 °C. The measured *intramolecular* exchange rates (Table 3) of 8 s^{-1} at 20 °C and 21 s^{-1} at 30 °C in THF are coherent with the reported[12] figure of 22 s^{-1} at 24 °C in toluene−CH_2Cl_2, suggesting that no significant solvent effect is involved. Neither the conventionally present paramagnetic impurity[1c,2,12] nor extra PPh_3 had an observable influence on this intramolecular exchange, for which activation parameters were determined: $E_a = 16.3 \pm 0.2$ kcal mol^{-1}, $\Delta G^{\ddagger} = 15.9$ kcal mol^{-1} (calculated at 20 °C), $\Delta H^{\ddagger} = 15.7 \pm 0.2$ kcal mol^{-1}, and $\Delta S^{\ddagger} = -0.8 \pm 0.8$ eu.

The *intermolecular* exchange mechanism was evaluated by consideration of the exchange matrix[27] describing the process, as in a previously reported and methodologically similar case.[28]

(27) Johnson, C. S.; Moreland, C. G. *J. Chem. Educ.* **1973**, *50*, 477.

Table 3. Intramolecular Exchange Rates for $[(Ph_3P)_3Rh(Cl)]$ in THF-d_8[a]

temp, °C	k_1,[b] s^{-1}
50	113 (4.2)
40	49.9 (1.04)
30	20.8 (0.23)
20	8.14 (0.23)
20	8.32 (0.13)[c,d]
20	8.27 (0.11)[c,e]
10	3.15 (0.04)
10	3.34 (0.10)[c,d]
10	3.10 (0.06)[c,e]
0	1.05 (0.03)

[a] In the presence of ca. 8 equiv of PPh_3. Unless specified otherwise, data are from the original sample of $[(Ph_3P)_3Rh(Cl)]$ prepared by the standard procedure and hence containing the paramagnetic impurity.[1c] [b] Standard deviation in parentheses. [c] Paramagnetic impurity-free sample (see the Experimental Section). [d] With ca. 7-fold excess PPh_3. [e] With ca. 2-fold excess PPh_3.

It was clear from Brown's[12] and our own work that this *intermolecular* exchange with free PPh_3 is significantly *slower* than *intramolecular* phosphine exchange in $[(Ph_3P)_3Rh(Cl)]$. A question that arose then was whether a site preference for intermolecular exchange could be distinguished, or if the rapid intramolecular exchange renders this question moot. An effort was made to address this issue experimentally by keeping the selective inversion pulse as short as possible so as to minimize the opportunity for exchange occurring during the inversion pulse time period. Since the duration of the selective inversion pulse is inversely proportional to its bandwidth, the bandwidth was increased to an extent such that the inversion bandwidth was no longer centered on the peak to be inverted. The criteria involved in judging the appropriateness of the inversion pulse included the extent of inversion (approximately 90%) and minimal impact on the intensity of the noninverted peaks. Typical bandwidths obtained by these criteria were 5−7 kHz, with corresponding pulse times ranging from 0.6 to 1.2 ms.

The first mechanism considered involved intermolecular exchange occurring between free PPh_3 and coordinated P_b (trans to Cl) at rate k_{2b}, in addition to the intramolecular process converting P_a (mutually trans phosphines) and P_b occurring at rate k_1. The data sets obtained at 30 °C are representative and are discussed here in detail; analogous results were obtained at the other temperatures. It was found that at 30 °C, $k_1 = 21.82 \pm 0.49\ s^{-1}$, and $k_{2b} = 2.74 \pm 0.09\ s^{-1}$. The second mechanism involved intermolecular exchange occurring at site P_a with rate constant k_{2a} and led to $k_1 = 20.78 \pm 0.23\ s^{-1}$ and $k_{2a} = 2.85 \pm 0.04\ s^{-1}$. The standard deviations for the latter model are seen to decrease by approximately a factor of 2. More dramatically however, the exchange model involving P_a was associated with a 75% decrease in the residual sum of squares compared with the model involving P_b.

Differences between the exchange models may also be discerned visually by examining the early time course of magnetization transfer. For example, Figure 3 shows the response of PPh_3 following selective inversion of site P_a and the least-squares result (solid line) for direct exchange between P_a and PPh_3. The dashed line is the least-squares result obtained for the model involving direct intermolecular exchange from site P_b following intramolecular exchange between P_b and the inverted site P_a. This putative indirect exchange between P_a and

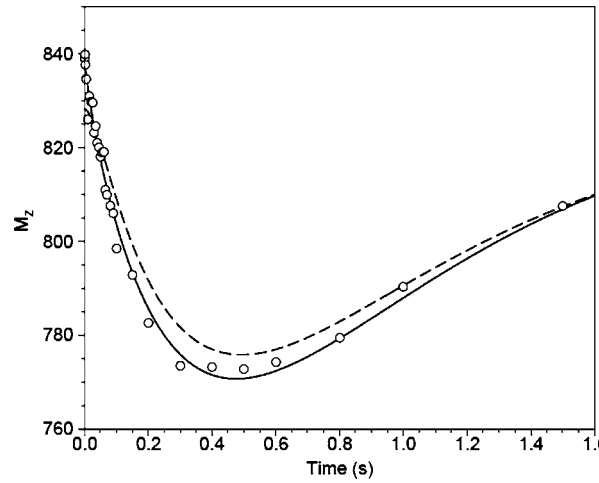

Figure 3. Time dependence of free PPh_3 magnetization (○) following selective inversion of site P_a. The model for direct P_a/PPh_3 exchange leads to the best-fitting least-squares result given by the solid line, whereas the model for direct P_b/PPh_3 exchange leads to the dashed line. The integral value for PPh_3 arises from setting the integral for P_b to 100.

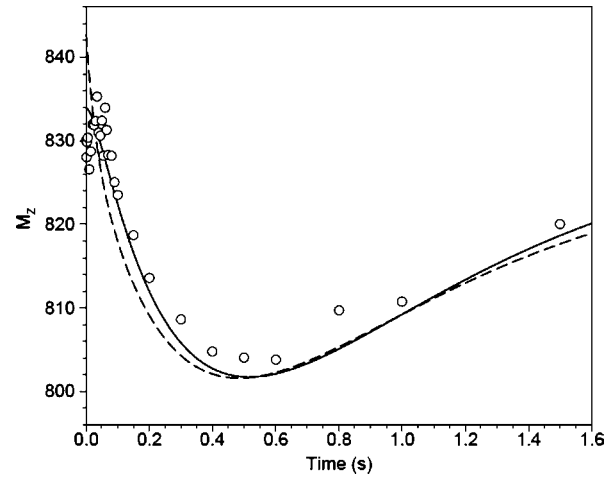

Figure 4. Time dependence of free PPh_3 magnetization (○) following selective inversion of site P_b. The meaning of the solid and dashed lines is the same as given in Figure 3.

PPh_3 leads to a delay in the modeled transfer of magnetization and to an estimated integrated intensity of 828 (Figure 3) at time 0, which is in contrast to the integrated intensity of 838 at time 0 for the direct P_a/PPh_3 exchange mechanism. The discrepancies between the dashed line and the experimental points contribute to the larger residual sum of squares observed for the model of intermolecular exchange occurring from site P_b.

The delay just mentioned can be observed for the response of PPh_3 following selective inversion of site P_b (Figure 4). In this case, the putative direct exchange between P_b and PPh_3 (dashed line) leads to an immediate decrease in the modeled magnetization intensity (estimated integrated intensity of 842 at time 0), while the delay in transfer of magnetization that proceeds from P_b to P_a and then to PPh_3 is both evident in the experimental data and better fit by the direct P_a/PPh_3 exchange model (solid line, estimated integrated intensity of 834 at time 0). Similar results are shown in Figure 5 for the exchange at sites P_a and P_b following selective inversion of PPh_3. The incorrect model (dashed line) clearly overestimates the exchange at P_b and underestimates the exchange at P_a.

(28) Roe, D. C.; Marshall, W. J.; Davidson, F.; Soper, P. D.; Grushin, V. V. *Organometallics* **2000**, *19*, 4575.

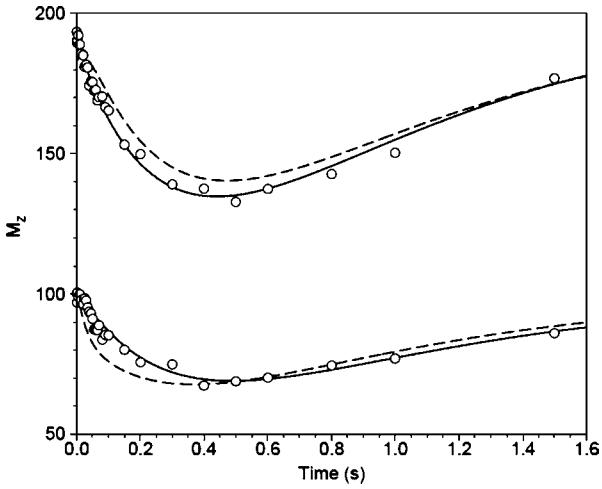

Figure 5. Time dependence of P_a (above) and P_b (below) magnetization (○) following selective inversion of free PPh_3. The meaning of the solid and dashed lines is the same as given in Figure 3.

Table 4. Intermolecular Exchange Rates for $[(Ph_3P)_3Rh(Cl)]$ in THF-d_8[a]

temp, °C	k,[b] s^{-1}
50	20.2 (0.53)
40	7.60 (0.13)
30	2.85 (0.04)
20	0.980 (0.044)
10	0.310 (0.012)
0	0.086 (0.009)

[a] In the presence of ca. 8 equiv of PPh_3. Data from the original sample of $[(Ph_3P)_3Rh(Cl)]$ prepared by the standard procedure and hence containing the paramagnetic impurity.[1c] [b] Standard deviation in parentheses.

It might be considered that intermolecular exchange at site P_a is preferred but that an independent exchange is also occurring via site P_b. This possibility was addressed by evaluating an exchange process that simultaneously included intramolecular exchange (k_1), intermolecular exchange at site P_b (k_{2b}), and intermolecular exchange at site P_a (k_{2a}). Since least-squares results may be influenced by the choice of initial guesses for parameters, it was decided to test the sensitivity of the mechanism to the fitting procedure by setting the initial guess for k_{2b} to be significantly larger than that for k_{2a}, even though the latter exchange process appears to be favored. For example, starting from $k_{2a} = 1.5\ s^{-1}$ and $k_{2b} = 9.0\ s^{-1}$, convergence was obtained for $k_1 = 20.76 \pm 0.24\ s^{-1}$, $k_{2a} = 2.79 \pm 0.11\ s^{-1}$, and $k_{2b} = 0.07 \pm 0.11\ s^{-1}$. This result was also associated with the same residual sum of squares found for the intermolecular exchange model involving P_a alone. Since the standard deviation for k_{2b} exceeded the parameter estimate, it was concluded that inclusion of this intermolecular process was immaterial for describing the overall exchange. This result indicates that for the conditions and temperature range studied, intermolecular exchange occurs exclusively from site P_a.[29]

Activation parameters were then determined for the intermolecular exchange (Table 4): $E_a = 19.0 \pm 0.3$ kcal mol^{-1}, $\Delta G^{\ddagger} = 17.2$ kcal mol^{-1} (calculated at 20 °C), $\Delta H^{\ddagger} = 18.5 \pm 0.3$ kcal mol^{-1}, and $\Delta S^{\ddagger} = 4.4 \pm 0.9$ eu. In contrast with the *intramolecular* rearrangement, *intermolecular* exchange between $[(Ph_3P)_3Rh(Cl)]$ and PPh_3 seems to be solvent-dependent: at 30 °C the rate of 2.9 s^{-1} in THF (this work; Table 4) is ca. 10 times higher than that in toluene−CH_2Cl_2 (0.31 s^{-1}).[12]

(29) In toluene-d_8, only R_3P (R = Ph, p-tolyl) trans to the IMes carbene ligand in *cis*-$[(R_3P)_2Rh(IMes)(Cl)]$ undergoes exchange with free phosphine, likely via a dissociative mechanism. See: Allen, D. P.; Crudden, C. M.; Calhoun, L. A.; Wang, R. *J. Organomet. Chem.* **2004**, *689*, 3203.

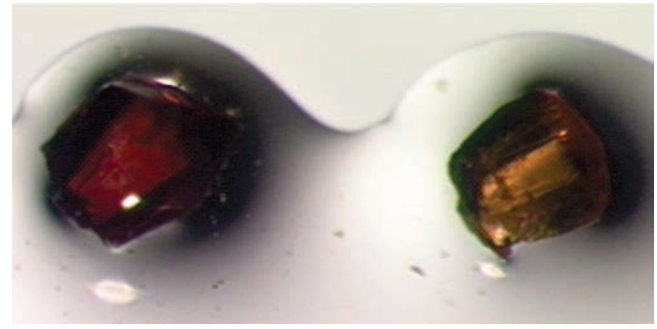

Figure 6. Single crystals of the red (left) and orange (right) forms of $[(Ph_3P)_3Ir(Cl)]$.

$[(Ph_3P)_3Ir(Cl)]$. While Wilkinson's catalyst has been structurally characterized and is known to exist in the orange and red polymorphic forms,[5] there have been no reports on single-crystal X-ray diffraction studies of its iridium counterpart. In their original full paper, Bennett and Milner[3c] indicated that by visual comparison of X-ray powder patterns, $[(Ph_3P)_3Ir(Cl)]$ was found to be isomorphous with the orange form of Wilkinson's catalyst, and that a red modification of $[(Ph_3P)_3Ir(Cl)]$ could not be made.

In order to obtain a better understanding of how the nature of the metal influences fluxionality of $[(Ph_3P)_3M(X)]$ (M = Rh, Ir), we also studied the iridium complex. Crystallization of $[(Ph_3P)_3Ir(Cl)]$ from benzene−hexanes produced orange-yellow crystals of X-ray quality that were analyzed and found to be isostructural with the orange form of Wilkinson's catalyst.[5] To reassure purity for solution studies, a freshly made batch of $[(Ph_3P)_3Ir(Cl)]$ was then recrystallized by addition of hexanes to its concentrated solution in THF. This, to our surprise, produced crystals that were homogeneously burgundy-red in color. When a portion of these red crystals was recrystallized again, in the same manner from a less concentrated solution, growth of both orange (major) and red (minor) crystals was observed (Figure 6). Unit cell parameters of one of the orange crystals matched those in the previous determination. X-ray diffraction of one of the red crystals revealed a different polymorph of $[(Ph_3P)_3Ir(Cl)]$ that was found to be isostructural with the red form of Wilkinson's catalyst. The structures of the two allotropes of $[(Ph_3P)_3Ir(Cl)]$ are shown in Figures 7 and 8.

As can be seen from Table 5, the red and orange forms of $[(Ph_3P)_3Ir(Cl)]$ exhibit coordination geometry parameters that are nearly identical to those of the corresponding forms of Wilkinson's catalyst. Within the MP_3Cl framework, the molecules are virtually pairwise superimposable. Both red polymorphs are notably more distorted away from the ideal square-planar geometry than the orange forms. The Bennett−Donaldson detailed analysis[5] of the structures of the red and orange forms of Wilkinson's catalyst is fully applicable to the structures of $[(Ph_3P)_3Ir(Cl)]$. This even includes the position and lengths of the nonprimary contacts of the metal centers with ortho-H atoms of the phenyl substituents, i.e. 2.89 Å (Ir) vs 2.84 Å (Rh)[5] for the orange forms and 2.84 Å (Ir) vs 2.77 Å (Rh)[5] for the red polymorphs.

At 20 °C, both intra- and intermolecular phosphine exchange of $[(Ph_3P)_3Ir(Cl)]$ in the presence of extra PPh_3 appeared to be too slow for detection (<0.01 s^{-1}). At 60 °C, only very sluggish

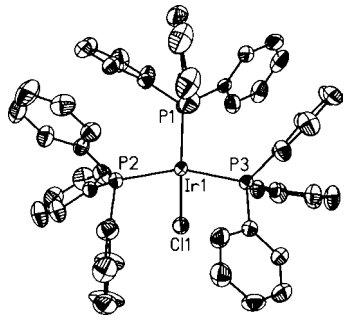

Figure 7. ORTEP drawing of the red form of $[(Ph_3P)_3Ir(Cl)]$.

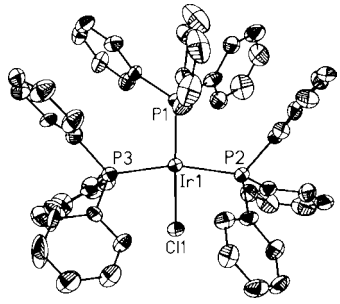

Figure 8. ORTEP drawing of the orange form of $[(Ph_3P)_3Ir(Cl)]$.

Table 5. Selected Coordination Geometry Parameters for the Red and Orange Forms of Wilkinson's Catalyst[5] and $[(Ph_3P)_3Ir(Cl)]$ (This Work) and Equivalent Parameters Computed with the BP86 Functional

	$[(Ph_3P)_3M(Cl)]$ red		$[(Ph_3P)_3M(Cl)]$ orange	
parameter	M = Ir (**2**)	M = Rh (**1**)	M = Ir (**2**)	M = Rh (**1**)
M−Cl (Å)				
X-ray	2.380(1)	2.376(4)	2.400(2)	2.404(4)
computed	2.44	2.42	2.45	2.42
M−P trans to Cl (Å)				
X-ray	2.198(1)	2.214(4)	2.219(2)	2.225(4)
computed	2.27	2.27	2.27	2.27
M−P trans to P (Å)				
X-ray	2.304(1)	2.322(4)	2.292(2)	2.304(4)
computed	2.35	2.35	2.35	2.35
M−P trans to P (Å)				
X-ray	2.310(1)	2.334(4)	2.318(2)	2.338(4)
computed	2.37	2.37	2.38	2.38
trans-Cl−M−P (deg)				
X-ray	158.0(1)	156.2(2)	167.4(1)	166.7(2)
computed	158.31	154.6	161.7	158.1
trans-P−M−P (deg)				
X-ray	153.0(1)	152.8(1)	159.2(1)	159.1(2)
computed	153.2	150.4	156.8	154.7

($0.7\ s^{-1}$) intramolecular and still no intermolecular exchange was observed. The cyclometalation that (unlike Wilkinson's catalyst) $[(Ph_3P)_3Ir(Cl)]$ undergoes[3c] already at 60 °C precluded the determination of activation parameters.

Computational Studies

Fluxionality of $[(R_3P)_3Rh(X)]$. As was mentioned above, the starting point of this work was the synthesis and study of the novel trifluoromethyl complex $[(Ph_3P)_3Rh(CF_3)]$, **3**. The uncommonly facile intramolecular phosphine exchange in **3** prompted us to investigate the mechanism of this process using density functional theory calculations and to compare this system with other $[(Ph_3P)_3Rh(X)]$ species that show different degrees of fluxionality. In our calculations we considered both $[(H_3P)_3Rh(X)]$ model species and the full $[(Ph_3P)_3Rh(X)]$ systems, and we focus initially on the case of $[(H_3P)_3Rh(CF_3)]$, **3′**, calculated with the BP86 functional.

Computed bond lengths for **3′** agree well with those of **3** (compare the data in Figures 9 and 2), although the distortion from square-planar observed experimentally is not reproduced due to the use of PH_3 ligands (see below). The reaction profile for phosphine exchange was investigated by reducing the *trans*-C−Rh−P1 angle in $\mathbf{3'_1}$ (where the subscript indicates CF_3 is initially trans to P1). This led to transition state $\mathbf{TS(3'\text{-}I')_1}$ ($E = +12.7$ kcal mol^{-1}) where CF_3 lies above the coordination plane (P1−Rh−C = 105°) and the *cis*-phosphines move toward the vacant site (P2−Rh−P3 = 130°). $\mathbf{TS(3'\text{-}I')_1}$ links to intermediate **I′** ($E = +11.5$ kcal mol^{-1}) which resembles a trigonal bipyramid (TBP) with a vacant axial site trans to CF_3. The near C_{3v} geometry of **I′** means that three equivalent transition states can be accessed by increasing the relevant C−Rh−P angles: $\mathbf{TS(3'\text{-}I')_1}$ returns CF_3 trans to P1, while $\mathbf{TS(3'\text{-}I')_2}$ and $\mathbf{TS(3'\text{-}I')_3}$ place CF_3 trans to P2 (as shown in Figure 9) and P3, respectively. $\mathbf{TS(3'\text{-}I')_{1/2/3}}$ are therefore high points on an energy surface that equilibrates all three phosphine ligands in **3′** with (for the BP86 functional) $\Delta H^{\ddagger}_{calcd} = 12.7$ kcal mol^{-1}.

Calculations on the full $[(Ph_3P)_3Rh(CF_3)]$ system indicate a very similar topology for the phosphine exchange surface. However, a considerable distortion away from square-planar is now computed for **3** (C−Rh−P1 = 144°, P2−Rh−P3 = 142°), more in accord with the experimental data in Figure 2. The reactant is thus distorted toward the transition state geometry with the result that the computed barrier is now only 4.0 kcal mol^{-1}. The bulkier PPh_3 ligands therefore facilitate exchange, but $\Delta H^{\ddagger}_{calcd}$ is significantly below the estimated[15,30] experimental value of 11.3 kcal mol^{-1}. This result was independent of functional and basis set choice, but an improved value of 8.7 kcal mol^{-1} was obtained when the energies of the BP86-optimized species were recomputed at the MP2 level. The good performance of the MP2//BP86 method was also seen for $[(Ph_3P)_3Rh(Me)]$ ($\Delta H^{\ddagger}_{calcd} = 14.8$ kcal mol^{-1} cf. 16.0 ± 0.6 kcal mol^{-1} from experiment) and for $[(Ph_3P)_3Rh(H)]$ ($\Delta H^{\ddagger}_{calcd} = 9.4$ kcal mol^{-1} cf. 10.3 ± 0.2 kcal mol^{-1} from experiment). It is noteworthy that the experimental value for the hydride was determined *after* the computational study to confirm the validity of the method. The MP2//BP86 methodology was therefore adopted for a larger series of $[(R_3P)_3Rh(X)]$ complexes.

Table 6 lists $\Delta H^{\ddagger}_{calcd}$ for a range of $[(R_3P)_3Rh(X)]$ species. In each case, use of the full PPh_3 ligands significantly reduces the barrier, indicating that steric bulk has a general accelerating effect on the exchange process. For the full models, good agreement with observed trends in fluxionality is computed, with the low barriers for X = CF_3, Me, Ph, and H mirroring the experimental behavior of these systems. An intermediate barrier of 19.4 kcal mol^{-1} was computed for X = CN, and experimental ^{31}P NMR spectra of $[(Ph_3P)_3Rh(CN)]$ do not show obvious signs of exchange at room temperature.[31] Relating $\Delta H^{\ddagger}_{calcd}$ to fluxionality rates assumes similar entropic changes for all X. Although entropy changes are difficult to address accurately in

(30) This estimated value of $\Delta H^{\ddagger} \approx 11.3$ kcal mol^{-1} for **3** was calculated using the exchange rate of 12.1 s^{-1} measured for **3** at −100 °C and $\Delta S^{\ddagger} = 12.7 \pm 2.5$ eu determined for $[(Ph_3P)_3Rh(CH_3)]$ (see above) under the careful assumption of similar entropies of activation for exchange in the two complexes.[15]

(31) Fernandes, M. A.; Circu, V.; Weber, R.; Varnali, T.; Carlton, L. *J. Chem. Crystallogr.* **2002**, *32*, 273.

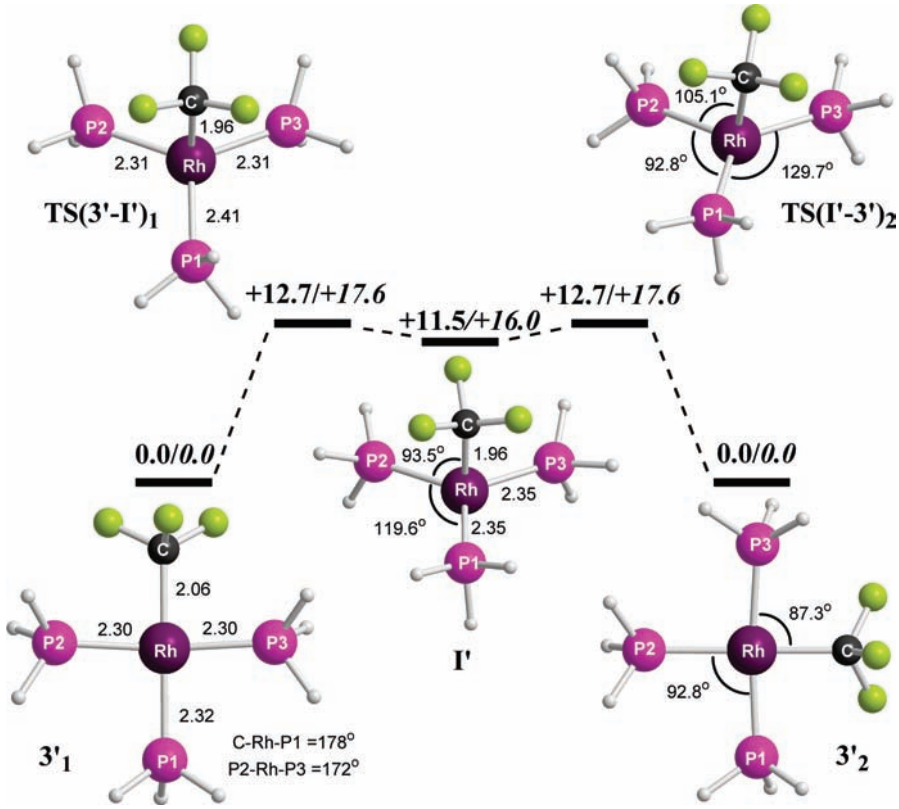

Figure 9. Computed reaction profile (kcal mol^{-1}) for intramolecular phosphine exchange in **3′** with selected distances and angles (Å, deg). **3′**$_1$/**3′**$_2$ and **TS(3′-I)**$_1$/**TS(3′-I)**$_2$ are structurally equivalent, with the subscript indicating the P center trans to the CF_3 group. Energies in italics are computed at the MP2//BP86 level (see text for details).

Table 6. $\Delta H^{\ddagger}_{calcd}$ (MP2//BP86, kcal mol^{-1}) for [$(R_3P)_3$Rh(X)]

	X					
	CF_3	Me	Ph	H	CN	Cl
R = H	17.6	19.9	21.2	12.7	28.2	48.5
R = Ph	8.7	14.8	12.5	9.4	19.4	N/A

present calculations due to the absence of solvent effects, generally, $\Delta S^{\ddagger}_{calcd}$ takes a small positive value, possibly due to the greater space available to the PPh_3 ligands in the transition state. One exception, however, was [$(Ph_3P)_3$Rh(H)] where a small negative $\Delta S^{\ddagger}_{calcd}$ was computed, and this is in full accord with the experimental value of -7.2 ± 0.8 eu that was determined as part of this study.

In the case where X = Cl, an exchange transition state could only be located for the [$(H_3P)_3$Rh(Cl)] model system, and moreover, this had a very high energy of 48.5 kcal mol^{-1}. With the full [$(Ph_3P)_3$Rh(Cl)] system, no evidence for an exchange transition state (or any trigonal intermediate) was obtained. Although the bulky PPh_3 ligands would be expected to reduce the computed exchange barrier from 48.5 kcal mol^{-1}, it seems unlikely that this would be sufficient to produce a value consistent with the ambient temperature exchange that is observed for [$(Ph_3P)_3$Rh(Cl)]. It is proposed therefore that intramolecular exchange in Wilkinson's catalyst might be governed by a different mechanism from that described above. Previously we had noted[15] that the triplet form of [$(R_3P)_3$Rh(Cl)] species may be reasonably accessible.[32] We therefore postulated that intramolecular phosphine exchange in **1** may occur via a spin crossover mechanism involving triplet [$(Ph_3P)_3$Rh(Cl)] as an intermediate. This possibility is investigated below, where we also extend our study to the [$(Ph_3P)_3$Ir(Cl)] analogue, **2**.

Intramolecular Phosphine Exchange in [$(Ph_3P)_3$Rh(Cl)] and [$(Ph_3P)_3$Ir(Cl)]. As a starting point for our calculations, we used the BP86 functional to compute two structures for both **1** and **2**, where the starting geometries were based on the red and orange forms in each case (see Table 5 for comparison with experimental data). For both metals, the two optimized structures were very close in energy, with the red form being marginally more stable, by ca. 0.4 kcal mol^{-1} in each case. The calculations consistently overestimate the M−ligand bond distances by ca. 2−3%, although trends are well-reproduced, with the M−P distances trans to Cl being 0.08−0.11 Å shorter than those cis to Cl. The *trans*-P−M−Cl and *trans*-P−M−P angles are in general slightly underestimated, although the greater degree of distortion away from planarity seen in the red forms is maintained in the calculations.

Subsequent calculations were based on the red form of [$(Ph_3P)_3$Rh(Cl)], the singlet form of which, ^{1}**1**, is assigned a relative energy of 0.0 kcal mol^{-1}. The triplet structure, ^{3}**1**, is computed with the BP86 functional to be only 15.4 kcal mol^{-1} higher in energy and exhibits a distorted tetrahedral geometry (P1−Rh−Cl = 101.7°, P2−Rh−P3 = 143.1°) in which all the Rh−ligand bonds are elongated compared to those in ^{1}**1** (see Figure 10). This is consistent with the occupation of formally σ-antibonding orbitals in the higher spin state structure. The energy profile for intramolecular exchange in [$(Ph_3P)_3$Rh(Cl)] is shown in Figure 10 (where the subscripts indicate which P center is trans to Cl). Narrowing the *trans*-P1−Rh−Cl angle in ^{1}**1**$_1$ leads to a rapid increase in energy with no evidence for any

(32) This was based on the small model system, [$(H_3P)_3$Rh(Cl)], where a distorted tetrahedral triplet was only 22.7 kcal mol^{-1} above the singlet ground state.[15]

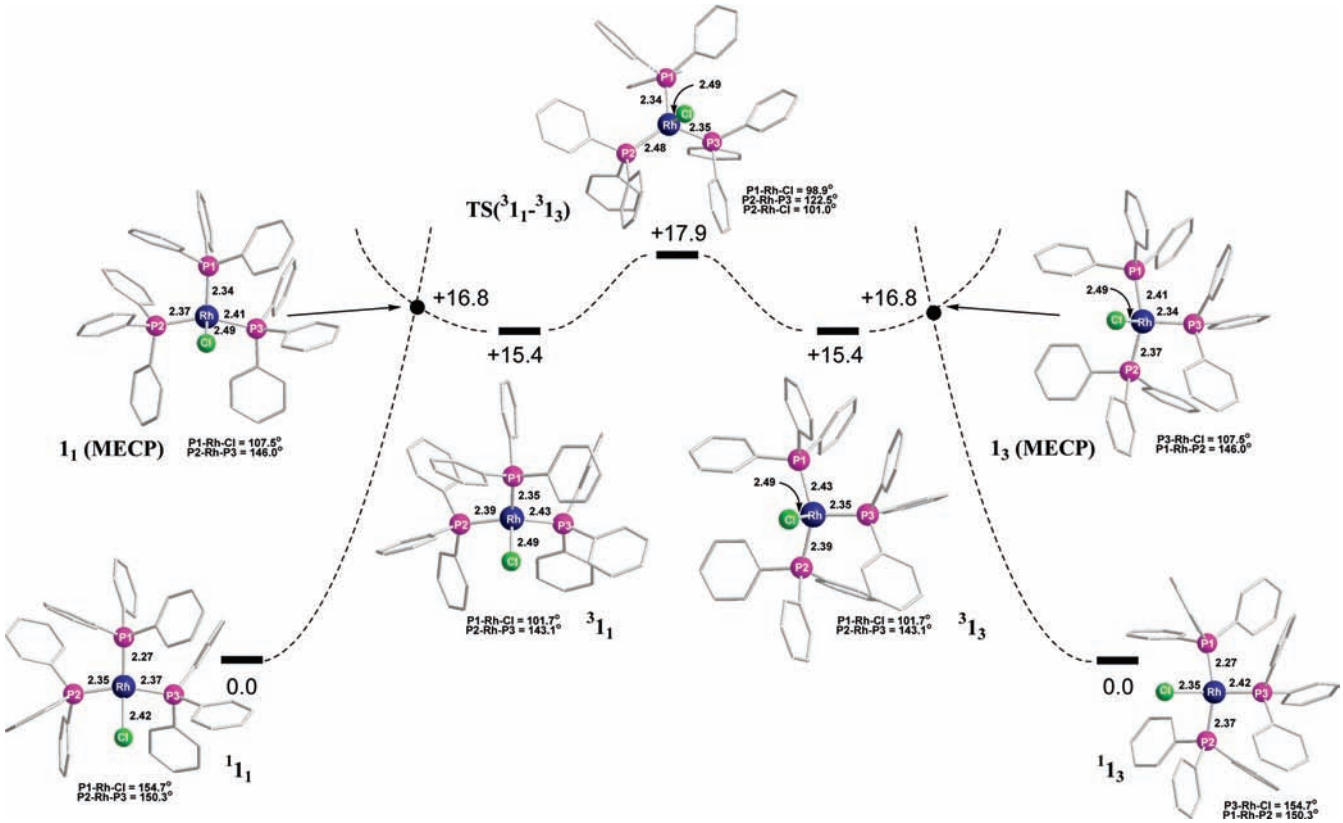

Figure 10. Computed reaction profile (BP86, kcal mol^{-1}) for intramolecular PPh_3 exchange in **1** with selected distances (Å) and angles (deg).

intermediate on the singlet surface being seen. Computation of a similar profile derived from $^3\mathbf{1}_1$, but now based on increasing the P1−Rh−Cl angle, also shows a steady increase in energy. Comparison of geometries and energies along these two profiles, however, does allow us to locate a minimum energy crossing point[33] between the two spin states ($\mathbf{1}_1$**(MECP)**, $E = +16.8$ kcal mol^{-1}).[34] $\mathbf{1}_1$**(MECP)** has a very similar geometry to $^3\mathbf{1}_1$ (P1−Rh−Cl = 107.5°, P2−Rh−P3 = 146.0°) and allows a low-energy route linking $^1\mathbf{1}_1$ to $^3\mathbf{1}_1$ to be defined. To further the overall exchange process, rearrangement of $^3\mathbf{1}_1$ is required in order to exchange the PPh_3 sites in this species. This was achieved by opening the P1−Rh−P2 angle and the location of a pseudo-C_{2v} transition state, **TS(**$^3\mathbf{1}_1$-$^3\mathbf{1}_3$**)** ($E = +17.9$ kcal/mol), with a P2−Rh−Cl angle of 101.0° and very similar values for P2−Rh−P3 (122.5°) and P2−Rh−P1 (125.2°). **TS(**$^3\mathbf{1}_1$-$^3\mathbf{1}_3$**)** leads to $^3\mathbf{1}_3$, an equivalent form of $^3\mathbf{1}_1$ in which P1 with P3 have exchanged positions. PPh_3 exchange is then completed via $\mathbf{1}_3$**(MECP)** to give $^1\mathbf{1}_3$ (these structures being equivalent to $\mathbf{1}_1$**(MECP)** and $^1\mathbf{1}_1$ seen in the initial steps of the process). The overall barrier to intramolecular phosphine exchange is therefore 17.9 kcal mol^{-1}, with the highest energy point involving rearrangement of the triplet intermediate via **TS(**$^3\mathbf{1}_1$-$^3\mathbf{1}_3$**)**. This barrier is in reasonable agreement with that determined experimentally (15.7 ± 0.2 kcal mol^{-1}).[35]

We also recomputed the energetics of this phosphine exchange in **1** at the MP2//BP86 level and found that both the singlet−triplet gap and the overall barrier via **TS(**$^3\mathbf{1}_1$-$^3\mathbf{1}_3$**)** increase significantly to 25.8 kcal mol^{-1} and +29.8 kcal mol^{-1}, respectively. The overall barrier is therefore about 12 kcal mol^{-1} above the experimental value, so it appears that for this intramolecular/spin crossover mechanism, it is the BP86 approach that provides more realistic energetics.

For $[(Ph_3P)_3Ir(Cl)]$, the triplet form, $^3\mathbf{2}$, was found with the BP86 functional to be 21.0 kcal/mol higher in energy than the singlet ground state. This larger singlet−triplet gap is to be expected when a third row species is compared with its second row congener. Rearrangement of $^3\mathbf{2}$ takes place in a similar fashion to $^3\mathbf{1}$, and the transition state involved has an energy of +24.4 kcal mol^{-1}. The barrier to intramolecular phosphine exchange in $[(Ph_3P)_3Ir(Cl)]$ is therefore 6.2 kcal mol^{-1} higher than that in $[(Ph_3P)_3Rh(Cl)]$,[36] consistent with the nonobservation of intramolecular exchange experimentally at room temperature.

Intermolecular Phosphine Exchange in $[(Ph_3P)_3Rh(Cl)]$ and $[(Ph_3P)_3Ir(Cl)]$. PPh_3 dissociation energies in **1** and **2** have also been computed to model the initial step in the intermolecular PPh_3 exchange process (Table 7). Although the rate of this exchange process is apparently solvent-dependent, the calculations can nonetheless provide information on the relative M−PPh_3 bond strengths. For both systems, dissociation of a *cis*-M−PPh_3 bond is computed to be significantly more facile

Table 7. Computed PPh_3 Ligand Dissociation Energies (BP86, kcal mol^{-1}) from **1** and **2**

	M = Rh	M = Ir
M−PPh_3 (trans)	22.0	36.2
M−PPh_3 (cis)	13.9	18.4[a]

[a] Slightly different values were obtained depending on which phosphine was removed, and an average result is given.

(33) Harvey, J. N.; Aschi, M.; Schwarz, H.; Koch, W. *Theor. Chem. Acc.* **1998**, *99*, 95.

(34) The MECP is not a stationary point, so the reported energy does not include any correction for zero-point energy. For comparison, the relative electronic energies of ^{3}**1** and **TS(**$^3\mathbf{1}$-$^3\mathbf{1}'$**)** are 16.1 and 19.0 kcal mol^{-1} respectively.

Table 8. Rh−P Bond Distances (Å) and Angles (deg) for Crystallographically Characterized Complexes [(Ph$_3$P)$_3$Rh(X)][a]

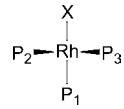

X	Rh−P1	Rh−P2	Rh−P3	s-angle[b]	X−Rh−P1	P2−Rh−P3	X−Rh−P3	P3−Rh−P1	P1−Rh−P2	P2−Rh−X	ref
H[c]	2.316	2.262	2.27	N/A	N/A	151.7	N/A	104.2	102.3	N/A	11
H[d]	2.288	2.245	2.279	8.0	172.1	147.3	78.2	102.8	109.9	69.2	41
H[d]	2.308	2.259	2.245	27.9	156.4	152.2	72.7	101.7	103.9	87.6	42
F	2.193	2.325	2.325	21.9	166.9	159.7	85.5	96.2	95.8	86.5	17
Cl (R)[e]	2.214	2.335	2.322	33.0	156.2	152.9	86.1	100.4	97.8	85.3	5
Cl (O)[f]	2.225	2.338	2.304	21.4	166.7	159.1	85.3	97.7	96.5	84.5	5
CN	2.315	2.297	2.343	28.6	159.3	155.8	84.9	98.0	98.9	85.3	31
PhO	2.228	2.348	2.312	27.6	164.7	152.3	79.2	99.1	99.2	88.2	18a
PhCO$_2$	2.210	2.326	2.343	14.4	172.0	161.3	79.1	98.5	96.6	87.4	43
NO$_3$	2.213	2.308	2.351	15.0	169.1	162.6	79.0	97.0	96.6	89.5	44
CF$_3$	2.313	2.310	2.337	27.6	163.5	156.5	88.6	94.5	96.4	86.9	15
CH$_3$	2.282	2.280	2.292	31.3	158.6	151.3	84.4	99.8	100.7	83.8	*g*

[a] P atoms of the P2−Rh−P3 fragment are projecting toward the reader with the Rh atom being in the plane of the page. [b] Interplanar angle between P1−Rh−P2 and X−Rh−P3. [c] Hydride not located. [d] Hydride located. The geometry parameters involving the hydride may deviate from the actual values because of the well-known inaccuracy of X-ray determination of hydrides on heavy metal centers. [e] Red form. [f] Orange form. [g] This work. Although the structure is of poor quality (see above), the geometry parameters listed for this complex herein are sufficiently reliable to be used in the discussion.

than a *trans*-M−PPh$_3$ bond. Contributions to this *cis*-labilization may arise from the higher trans influence of PPh$_3$ compared with Cl and the presence of a cis π-donor ligand,[37] both features that may weaken the *cis*-M−PPh$_3$ interaction. In addition, the 3-coordinate species formed upon loss of a *cis*-PPh$_3$ has a vacant site cis to Cl, which may allow for a greater degree of π-stabilization of the 14e intermediate formed. Dissociation of the *cis*- and *trans*-Ir−PPh$_3$ bonds is much harder than the equivalent Rh−PPh$_3$ bonds. The calculations therefore again reproduce the trends seen experimentally that indicate more facile dissociation of a *cis*-PPh$_3$ ligand in [(Ph$_3$P)$_3$Rh(Cl)] as well as the greatly reduced lability in [(Ph$_3$P)$_3$Ir(Cl)].

Interestingly, a quantitative comparison of the computed results for the intra- and intermolecular exchange processes is less successful. Assuming that the *cis*-M−PPh$_3$ dissociation energy in [(Ph$_3$P)$_3$Rh(Cl)] represents a lower limit for the barrier to intermolecular exchange, then the calculations predict this process ($\Delta E^{\ddagger}$ = 13.9 kcal mol^{-1}) to be more accessible than intramolecular exchange ($\Delta E^{\ddagger}$ = 17.9 kcal mol^{-1}) (and this is even before entropic effects, which should further favor the dissociative process, are taken into account). That such difficulties are encountered is perhaps not surprising. For example, computation of M−PPh$_3$ binding energies has recently been shown to be highly dependent on the approach adopted, with pure and hybrid GGA functionals tending to underestimate the magnitude of the interaction.[38] This may arise from the well-known underestimation of dispersion effects by these methods. More recent functionals, such as Truhlar's M06 family,[39] or approaches that directly include an empirical correction for dispersion effects[40] have shown greatly improved performance in this respect. For the present system, use of the M06 functional did not produce any significant change in the computed geometry of **1**; however it did yield a much larger value of 35.6 kcal mol^{-1} for the *cis*-Rh−PPh$_3$ bond strength, more than twice the BP86 figure. Comparison between nondissociative and dissociative processes also requires an accurate assessment of entropic contributions and solvation effects. Thus, while the computation of the trends in reactivity *within* the intra- or intermolecular regimes provides good comparison with experiment, comparison *between* these two mechanisms remains a challenge.

Discussion

A number of [(Ph$_3$P)$_3$Rh(X)] bearing various X have been structurally characterized by single-crystal X-ray diffraction. All of these complexes exhibit deviation from ideal square-planar geometry. However, as may be seen from Table 8, there does not seem to be an obvious, well-pronounced correlation between the degree of this distortion in the crystalline state[45] and fluxionality of the species in solution. Our experimental and computational studies indicate that at least two different mechanisms can govern intramolecular phosphine exchange processes for [(Ph$_3$P)$_3$Rh(X)], pathway A involving a transition state resembling a trigonal bipyramid with a vacant axial site

(35) The overall rate of the intramolecular exchange process should not be significantly affected by the need to change spin state at the MECP. This is related to the magnitude of the spin-orbit coupling and so for a 2nd row transition metal such as Rh should be reasonably facile. In addition, under the experimental conditions employed here (0−50 °C) the enthalpic barrier represented by **TS(^{3}1$_1$-^{3}1$_3$)** is likely to dominate over the rate of surface crossing associated with the preceding lower energy MECP. See: Carreón-Macedo, J. L.; Harvey, J. N. *J. Am. Chem. Soc.* **2004**, *126*, 5789. Harvey, J. N. *Phys. Chem. Chem. Phys.* **2007**, *9*, 331. Besora, M.; Carreón-Macedo, J. L.; Cowan, A. J.; George, M. W.; Harvey, J. N.; Portius, P.; Ronayne, K. L.; Sun, X.-Z.; Towrie, M. *J. Am. Chem. Soc.* **2009**, *131*, 3583.

(36) We have not located MECPs for the singlet/triplet crossing in **2** but assume that the highest point in the intramolecular phosphine exchange profile will be equivalent to **TS(^{3}1$_1$-^{3}1$_3$)**, as seen for **1**.

(37) MacQueen, D.; Macgregor, S. A. *Inorg. Chem.* **1999**, *38*, 4868.

(38) Minenkov, Y.; Occhipinti, G.; Jensen, V. R. *J. Phys. Chem. A* **2009**, *113*, 11833.

(39) Zhao, Y.; Truhlar, D. G. *Acc. Chem. Res.* **2008**, *41*, 157.

(40) Grimme, S. *J. Comput. Chem.* **2006**, *27*, 1787.

(41) Hanusa, T. P.; Evans, W. J. *J. Coord. Chem.* **1986**, *14*, 223.

(42) Burgess, K.; Van der Donk, W. A.; Westcott, S. A.; Marder, T. B.; Baker, R. T.; Calabrese, J. C. *J. Am. Chem. Soc.* **1992**, *114*, 9350.

(43) Gusev, A. I.; Struchkov, Yu. T. *Zh. Strukt. Khim.* **1974**, *15*, 282.

(44) Heaton, B. T.; Iggo, J. A.; Jacob, C.; Blanchard, H.; Hursthouse, M. B.; Ghatak, I.; Harman, M. E.; Somerville, R. G.; Heggie, W. *J. Chem. Soc., Dalton Trans.* **1992**, 2533.

(45) For studies and discussions of factors influencing distortions in square-planar complexes, see, for example: (a) Rahn, J. A.; O'Donnell, D. J.; Palmer, A. R.; Nelson, J. H. *Inorg. Chem.* **1989**, *28*, 2631. (b) Magistrato, A.; Merlin, M.; Pregosin, P. S.; Rothlisberger, U.; Albinati, A. *Organometallics* **2000**, *19*, 3591.

Scheme 1

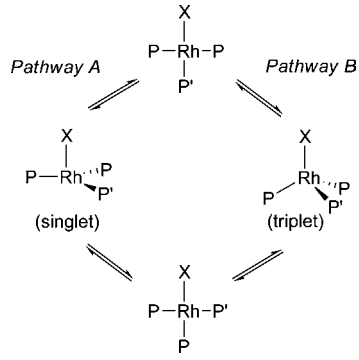

Table 9. Selected Computed Natural Atomic Charges for $[(H_3P)_3Rh(X)]$ Reactants and Transition States[a]

	reactants			transition states		
X	*q*(Rh)	*q*(C^{α}/X)	*q*(P_{avg})	*q*(Rh)	*q*(C^{α}/X)	*q*(P_{avg})
CF_3	−0.52	+0.79	+0.23	−0.26	+0.93	+0.08
Me	−0.48	−0.96	+0.23	−0.24	−0.73	+0.10
Ph	−0.48	−0.22	+0.24	−0.20	+0.03	+0.08
H	−0.63	−0.09	+0.22	−0.45	+0.14	+0.10
CN	−0.49	−0.02	+0.25	−0.17	+0.14	+0.10
Cl	−0.45	−0.52	+0.25	−0.08	−0.33	+0.10

[a] Other centers display only minor changes in computed charge.

trans to X (Scheme 1; Figure 9) and pathway B in which spin crossover leads to a pseudotetrahedral triplet intermediate (Scheme 1; Figure 10).[46]

Pathway A is operational for strong trans influence[47] X substituents that stabilize the transition state by electron donation. Indeed, most previously reported fluxional $[(Ph_3P)_3Rh(X)]$ systems (X = Me, H, Ph) feature strongly donating ligands. CF_3 is also considered a powerful trans influence ligand,[48,49] and this is confirmed by the Rh−P1 distance of 2.31 Å in **3**, which is as long as that measured in $[(Ph_3P)_3Rh(H)]$.[11] Figure 9 shows that as CF_3 moves into an axial position, trans to a developing vacant site, the Rh−C bond shortens considerably, implying greater donation to the metal center. Similar changes are seen for all X, but one would expect the greater donor ability characteristic of the highest trans influence ligands to offer the greatest stabilization and so produce lower barriers.

Validation of these ideas comes from computed natural atomic charges for the reactant and transition state structures, as shown in Table 9 for the simplified $[(H_3P)_3Rh(X)]$ models.[15] Transition state formation entails increased donation from the donor atom

Scheme 2

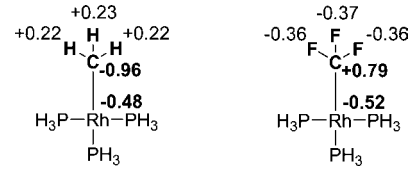

of X of around $0.2e^-$. Despite this, the e^- density on Rh actually diminishes in the transition state, and it is the P centers that ultimately receive the extra charge density. This can be understood if the near-trigonal transition states are considered to be a fragment of a trigonal bipyramid. Such a structure has two occupied d-orbitals with significant σ-antibonding interactions with the phosphine ligands (consistent with increased Rh−P distances in both $\mathbf{TS(3'\text{-}I')_1}$ and **I′** compared to **3′**, Figure 9). These d-orbitals are approximately σ-nonbonding in the square-planar reactant and so transition state formation entails a delocalization of e^- density onto the P centers, typically of about $0.15e^-$ each.[50] The loss of electron density at Rh can be mitigated by strong donation from X, and the highest charge density at Rh is found when X = CF_3, Me, H, and Ph, consistent with the high trans influence of these ligands. The lower charges on Rh in the transition state for X = CN (despite its strong trans influence[31,47]) and, especially, X = Cl correlate with the higher barriers computed in these cases.

While the strong trans influence of H, Me, and Ph has long been known, the electronic properties of the CF_3 group are not without controversy. In organic chemistry, the CF_3 group is widely recognized as a powerful electron acceptor.[51] In sharp contrast, the high trans influence of the CF_3 ligand[48,49] points to its strong electron donation that may be predominantly or exclusively controlled by σ-effects.[52] Indeed, X-ray structures of $[(dppe)Pd(CF_3)(Cl)]$ and $[(dppe)Pd(CH_3)(Cl)]$ have been found[49e] to exhibit almost identical coordination geometry parameters, including the lengths of the Pd−P bonds trans to the CF_3 (2.345(1) Å) and to the CH_3 (2.339(1) Å) ligands. Most importantly, calculations indicate that the Rh atom in $[(H_3P)_3Rh(X)]$ (Table 8) does bear a large negative charge for X = CF_3 (−0.52), exceeding that for X = CH_3 (−0.48), despite the opposite, strong charges on the carbon atoms of the CF_3 (+0.79) and the CH_3 (−0.96) ligands (Scheme 2).[53]

(46) Both transition states shown in Scheme 1 (for details, see Figures 9 and 10) are removed from C_3-type symmetry and hence do obey the selection rules for transition states of chemical transformations. See: McIver, J. W., Jr.; Stanton, R. E. *J. Am. Chem. Soc.* **1972**, *94*, 8618. Stanton, R. E.; McIver, J. W., Jr. *J. Am. Chem. Soc.* **1975**, *97*, 3632.

(47) Appleton, T. G.; Clark, H. C.; Manzer, L. E. *Coord. Chem. Rev.* **1973**, *10*, 335.

(48) For reviews, see: (a) Hughes, R. P. *Adv. Organomet. Chem.* **1990**, *31*, 183. (b) Morrison, J. A. *Adv. Organomet. Chem.* **1993**, *35*, 211.

(49) For discussions of the trans influence and trans effect of CF_3 and other polyfluoroalkyl ligands, see: (a) Bennett, M. A.; Chee, H.-K.; Robertson, G. B. *Inorg. Chem.* **1979**, *18*, 1061. (b) Bennett, M. A.; Chee, H.-K.; Jeffery, J. C.; Robertson, G. B. *Inorg. Chem.* **1979**, *18*, 1071. (c) Hughes, R. P.; Overby, J. S.; Williamson, A.; Lam, K.-C.; Concolino, T. E.; Rheingold, A. L. *Organometallics* **2000**, *19*, 5190. (d) Hughes, R. P.; Meyer, M. A.; Tawa, M. D.; Ward, A. J.; Williamson, A.; Rheingold, A. L.; Zakharov, L. N. *Inorg. Chem.* **2004**, *43*, 747. (e) Grushin, V. V.; Marshall, W. J. *J. Am. Chem. Soc.* **2006**, *128*, 4632. (f) See also: Yang, D. S.; Bancroft, G. M.; Puddephatt, R. J.; Tse, J. S. *Inorg. Chem.* **1990**, *29*, 2496.

(50) Albright, T. A.; Burdett, J. K.; Whangbo, M.-H. *Orbital Interactions in Chemistry*; John Wiley & Sons: New York, 1985.

(51) See, for example: (a) Hansch, H.; Leo, A.; Taft, R. W. *Chem. Rev.* **1991**, *91*, 165. (b) Uneyama, K. *Organofluorine Chemistry*; Blackwell: Oxford, U.K., 2006.

(52) Landis, C. R.; Firman, T. K.; Root, D. M.; Cleveland, T. *J. Am. Chem. Soc.* **1998**, *120*, 1842.

(53) (a) It is surprising that in a recent paper, perfluoroalkyl groups (including CF_3) are unambiguously viewed as "'hard' ligands with a marked electron-withdrawing ability".[53b] Even more surprisingly, in another recent publication, Vicic and co-workers[53c] arrive at the conclusion of "the extreme electron-withdrawing properties of the trifluoromethyl ligand" on the basis of electrochemical data, while apparently ignoring the facts that redox potentials are a purely thermodynamic parameter for a redox pair in a particular environment (solvent), and that in their own series of complexes [(BOXAM)Ni(X)], the X ligands CH_3, Ph, and CF_3 exhibit virtually the same structural trans influence: the Ni−N bond distances trans to X are 1.933(3), 1.939(2), and 1.921(3) Å for CH_3, Ph, and CF_3, correspondingly. (b) Menjón, B.; Martínez-Salvador, S.; Gómez-Saso, M. A.; Forniés, J.; Falvello, L. R.; Martín, A.; Tsipis, A. *Chem.—Eur. J.* **2009**, *15*, 6371. (c) Kieltsch, I.; Dubinina, G. G.; Hamacher, C.; Kaiser, A.; Torres-Nieto, J.; Hutchison, J. M.; Klein, A.; Budnikova, Y.; Vicic, D. A. *Organometallics* **2010**, *29*, 1451.

Scheme 3

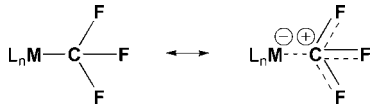

This charge distribution in [(H$_3$P)$_3$Rh(CF$_3$)], **3′**, resembles the long-known[54] β-effect in fluorinated organic molecules, where substitution of F for H on a carbon atom *increases* the negative charge on the next C (or H) atom. The explanation of the β-effect by π-donation from the F atoms[54a,c] accounts for the apparent flow of electrons toward the metal center in **3′** (Scheme 3). Nonetheless, the overall charge on the CF$_3$ and the CH$_3$ ligands is almost the same (−0.30 vs −0.29), and hence the CF$_3$ group, as a whole, should not be viewed as carbocationic.[55] These charge data (Table 9, Scheme 2) shed light on the previously perplexing strong trans influence of CF$_3$ and other perfluoroalkyl ligands.[48,49] Also, the electrostatic attraction resulting from the M$^{\delta-}$−$^{\delta+}$CF$_3$ polarization may, in certain cases, contribute to the M−C bond shortening in polyfluoroalkyl complexes,[48,49] compared with their nonfluorinated counterparts.[56] The positive charge on the carbon atom (Schemes 2 and 3) is likely stabilized by the p(π) back-donation mechanism from the fluorines.[54,55a] Both the charge distribution pattern (Scheme 2) and the proposed resonance form (Scheme 3) are consistent with the apparent weakening of the trans influence on displacement of the fluorine atoms on the CF$_3$ group with perfluoroalkyl groups[49a,c,d,57−59] that, unlike fluorine, do not exhibit strong π-donation.[51,60] In accord with this, [(Ph$_2$PMe)$_3$Rh(C$_3$F$_7$)] is less fluxional than [(Ph$_2$PMe)$_3$Rh(CF$_3$)].[16]

Pathway A is also influenced by steric factors, as is evident for all [(Ph$_3$P)$_3$Rh(X)] species in Table 6, with $\Delta H^{\ddagger}_{\mathrm{calcd}}$ always being lower than for the [(H$_3$P)$_3$Rh(X)] congeners. A number of experimental data support this. For instance, while intramolecular exchange in [(Ph$_3$P)$_3$Rh(CF$_3$)] is slow on the NMR time scale only at −100 °C and below (this work; see also ref 15), sharp lines are already observed at −40 °C in the ^{19}F and ^{31}P NMR spectra of [(Ph$_2$PMe)$_3$Rh(CF$_3$)].[16] In accord with this, [(Me$_3$P)$_3$Rh(Ph)][13] and *cis*-[(Ph$_3$P)$_2$(Ph$_2$PF)Rh(Ph)][14,61] are less fluxional than sterically more encumbered [(Ph$_3$P)$_3$Rh(Ph)]. The calculations also showed that the effect of introducing PPh$_3$ ligands into the model was most pronounced when combined with larger X groups, reducing the barrier by ca. 9 kcal mol^{-1} for X = CF$_3$ and Ph, by 5.1 kcal mol^{-1} for X = Me but by only 3.3 kcal mol^{-1} for X = H (see Table 6). Furthermore, judging only by the strongest negative charge on Rh (Table 9), one would expect the hydride [(Ph$_3$P)$_3$Rh(H)] to be the most fluxional species in the series. This is not the case, however, apparently due to the steric effect and negative entropy of activation that are counterdirecting and particularly significant for the small H ligand. Indeed, the entropy of activation for the intramolecular exchange via pathway A (Scheme 1) is a small positive figure, except for X = H where a small negative $\Delta S^{\ddagger}$ was first computed[15] and subsequently experimentally determined in this work (−7.2 ± 0.8 eu). In general, the greater space available to the phosphine ligands in the TS should result in positive $\Delta S^{\ddagger}$. The small yet *negative* $\Delta S^{\ddagger}$ observed for intramolecular exchange in [(Ph$_3$P)$_3$Rh(H)] might be, as we carefully propose, the consequence of the exceptionally small size of hydride, conceivably allowing for a less hindered and hence more rigid transition state.

While being feasible for strong trans influence X, pathway A is prohibitively high in energy when X is a weaker electron donor that is unable to sufficiently stabilize the near-trigonal transition state. In fact, a trigonal structure could not be located for Wilkinson's catalyst (**1**) where X = Cl. Nonetheless, **1** does undergo intramolecular phosphine exchange, as has been demonstrated earlier[10,12] and confirmed in this work. Our computational study indicates that this exchange, which is experimentally detected and quantified by NMR, is governed by a different, spin crossover mechanism involving a distorted tetrahedral triplet[62] [(Ph$_3$P)$_3$Rh(Cl)] as an intermediate (Scheme 1, pathway B).[63]

In parallel with intramolecular ligand exchange, **1** undergoes intermolecular exchange with free PPh$_3$, as follows from the previous studies[10,12] and this work. Unlike the intramolecular rearrangement, which is not influenced significantly by solvent (see above), the intermolecular exchange involving **1** and free PPh$_3$ seems to be solvent-dependent with the rate in CH$_2$Cl$_2$−toluene[12] being roughly 10 times slower than that in more coordinating THF (this work) at 30 °C. The small positive entropy of activation ($\Delta S^{\ddagger}$ = 4.4 ± 0.9 eu) and the lack of rate dependence on [PPh$_3$] are incoherent with an associative mechanism for intermolecular PPh$_3$ exchange, in full accord with the conclusion that Eaton and Suart arrived at as early as 1968.[10] Our experimental data for the first time answer the long-standing, intriguing question of which phosphine dissociates

(54) (a) Pople, J. A.; Gordon, M. *J. Am. Chem. Soc.* **1967**, *89*, 4253. (b) Davis, D. W.; Banna, M. S.; Shirley, D. A. *J. Chem. Phys.* **1974**, *60*, 237. (c) Holmes, S. A.; Thomas, T. D. *J. Am. Chem. Soc.* **1975**, *97*, 2337.

(55) (a) Christe, K. O.; Hoge, B.; Boatz, J. A.; Prakash, G. K. S.; Olah, G. A.; Sheehy, J. A. *Inorg. Chem.* **1999**, *38*, 3132. (b) Christe, K. O.; Zhang, X.; Bau, R.; Hegge, J.; Olah, G. A.; Prakash, G. K. S.; Sheehy, J. A. *J. Am. Chem. Soc.* **2000**, *122*, 481.

(56) (a) In general, this shortening is rationalized in terms of significant carbon 2s character in the M−CF$_3$ bonds.[48,49,53b] Note that in some cases, such as (CX$_3$)$_n$E (E = P, As; n = 3 and E = Hg, n = 2) the C−E bond is shorter for X = H than for X = F.[56b−d] (b) Yokozeki, A.; Bauer, S. H. *Top. Curr. Chem.* **1975**, *53*, 71. (c) Brauer, D. J.; Bürger, H.; Eujen, R. *J. Organomet. Chem.* **1977**, *135*, 281. (d) Liao, M.-S.; Huang, S.-P. D. *J. Organomet. Chem.* **2000**, *598*, 374.

(57) Hughes, R. P.; Sweetser, J. T.; Tawa, M. D.; Williamson, A.; Incarvito, C. D.; Rhatigan, B.; Rheingold, A. L.; Rossi, G. *Organometallics* **2001**, *20*, 3800.

(58) Hughes, R. P.; Ward, A. J.; Rheingold, A. L.; Zakharov, L. N. *Can. J. Chem.* **2003**, *81*, 1270.

(59) Care should be exercised to avoid overinterpretation of bond length data because of the difficulty of separating cis steric effects from the trans influence.[57]

(60) (a) A reviewer proposed a negative hyperconjugation[60b,c] structure as an alternative to the one shown in Scheme 3 to account for a low barrier pathway to the α-F-elimination (eq 1) and for the positive charge on C (Scheme 2) in **3**. Although such a negative hyperconjugation resonance structure may contribute to the overall system, it would not account for the strong negative charge on Rh (Table 9 and Scheme 1), because heterolysis of the C−F bond implies a removal of electron density from that site. The resonance forms implied in Scheme 3 would therefore appear to dominate in this case. (b) For an early discussion of negative hyperconjugation in benzotrifluorides, see: Roberts, J. D.; Webb, R. L.; McElhill, E. A. *J. Am. Chem. Soc.* **1950**, *72*, 408. (c) For a recent overview of negative hyperconjugation of CF$_3$ and some fluorine containing groups, see: Exner, O.; Böhm, S. *New J. Chem.* **2008**, *32*, 1449.

(61) Macgregor, S. A.; Wondimagegn, T. *Organometallics* **2007**, *26*, 1143.

(62) Cirera, J.; Ruiz, E.; Alvarez, S. *Inorg. Chem.* **2008**, *47*, 2871, and references therein.

(63) (a) The magnetic field (NMR) is not expected to have a significant effect on triplet state-mediated phosphine exchange in [(Ph$_3$P)$_3$Rh(Cl)].[63b] It is also worth emphasizing that in the NMR spectra we did not observe any unusual signs that would point to an influence of the electron spin in the triplet intermediate on the NMR experiments. (b) For a review of the spin crossover phenomenon under magnetic field, see: Bousseksou, A.; Varret, F.; Goiran, M.; Boukheddaden, K.; Tuchagues, J.-P. *Top. Curr. Chem.* **2004**, *235*, 65.

faster from **1**, clearly showing that it is one of the two mutually trans PPh_3 ligands that comes off the metal. Although this is fully consistent with the Rh−P bonds cis to Cl being 0.08−0.12 Å longer than the one trans to Cl (in the solid state),[5] care should be exercised in concluding that under the conditions used, a simple dissociative mechanism is operational. The aforementioned solvent effect for the intermolecular exchange suggests that the medium (THF) may be involved. It seems likely that $[(Ph_3P)_2Rh(Cl)]$ produced upon PPh_3 loss from **1** is stabilized by coordination with solvent molecules. If so, the intimate structure and stereochemistry of any solvento species involved remains unknown.

As expected, both intra- and intermolecular exchange in $[(Ph_3P)_3Ir(Cl)]$ (**2**) were found to be considerably slower than in its rhodium congener **1**. Intramolecular exchange in **2** could not be detected at room temperature (<0.01 s^{-1}) and was found to be slow (0.7 s^{-1}) at 60 °C. In accord with this, the computed barrier to intramolecular phosphine exchange in **2** (24.4 kcal mol^{-1}) is 6.2 kcal mol^{-1} higher than that in $[(Ph_3P)_3Rh(Cl)]$. No intermolecular exchange could be experimentally detected by the same magnetization transfer method for solutions of **2** in THF containing free PPh_3 in the temperature range of 20−60 °C.

Throughout these studies calculations have been used to provide insight into the different mechanisms of phosphine exchange. The range of processes involved presents a challenge to methodology, and different methods have been required to obtain realistic energetics in each case. Thus intramolecular exchange in $[(Ph_3P)_3Rh(X)]$ (X = CF_3, CH_3, Ph, H, CN) appears well described by the MP2//BP86 approach, presumably because the use of the MP2 approach provides a better treatment of the weak interactions associated with bulky PPh_3 ligands. This approach, however, overestimates the energetics of exchange in $[(Ph_3P)_3M(Cl)]$ (M = Rh, Ir), where a spin-crossover process is involved. The BP86 functional performs better in the latter case, but this method then severely underestimates M−PPh_3 binding energies and incorrectly suggests that intermolecular PPh_3 exchange might be more facile than the intramolecular process. The M06 functional appears more correct in this regard. Thus, although the calculations have provided valuable qualitative insight into each of the different reactions available to $[(Ph_3P)_3M(X)]$ systems, a single methodolgy to treat all these processes has yet to be identified. These systems therefore provide an excellent testing ground for different methodologies and work to define the best approach is underway in one of our groups (S.A.M.).

Conclusions and Outlook

Mechanisms of intramolecular and intermolecular ligand exchange in complexes of the type $[(R_3P)_3M(X)]$ (M = Rh, Ir) have been elucidated by experimental and computational methods. For the Rh complexes, the intramolecular exchange can be governed by at least two distinct mechanisms.

When X is a strong trans influence ligand (e.g., H, Me, Ph, CF_3), the rearrangement occurs via a distorted trigonal transition state with the anionic ligand X in an axial position trans to a vacant site (Scheme 1, pathway A). This exchange is governed by a combination of steric and electronic factors and is facilitated by bulkier ligands on the Rh, as well as by strongly donating anionic ligands X that can stabilize the transition state. The extremely fast intramolecular exchange observed for $[(Ph_3P)_3M(CF_3)]$ (**3**) is apparently brought about by the very strong electron donation from the CF_3 ligand to the metal center, as can be seen from the charge distribution study in **3′** and a number of its counterparts with various X. These results shed light on the previously puzzling strong trans influence of the CF_3 group which, in sharp contrast, is known to be a strong electron acceptor in organic chemistry.[51]

For weaker trans influencing ligands X, the near-trigonal transition state is insufficiently stabilized and hence reaction via this route can no longer be operational. As exemplified by Wilkinson's catalyst (**1**; X = Cl), the intramolecular exchange observed previously[10,12] and in this work occurs via a different, spin crossover mechanism involving a distorted tetrahedral triplet $[(Ph_3P)_3Rh(Cl)]$ as an intermediate (Scheme 1, pathway B). In parallel, **1** undergoes intermolecular exchange with free PPh_3 via a dissociative mechanism. The two exchange processes have been discerned and activation parameters determined for both. While PPh_3 loss from **1** has been long known and widely recognized as a key step in many reactions catalyzed by **1**,[1,2,4] our magnetization transfer experiments have allowed, for the first time, the determination of which phosphine dissociates faster from the Rh center: one of the two that are mutually trans. This important conclusion drawn from our experimental results is fully supported by our computational studies showing that PPh_3 dissociation from a position that is trans to another PPh_3 is significantly more accessible than from the position that is trans to Cl.[64] Unsurprisingly, both intramolecular and intermolecular exchange processes in the heavier analogue of **1**, the iridium complex **2**, occur at a much slower rate. We have also, for the first time, found that like **1**, **2** can exist in two crystallographic forms, orange and red, which are pairwise isostructural with those of **1**.

In this work, we have carried out kinetic studies of exchange in four complexes of the type $[(Ph_3P)_3Rh(X)]$ with X = H, CH_3, CF_3, and Cl. While it would be desirable to obtain similar data including activation parameters for other X in order to obtain a deeper understanding of the phosphine rearrangement processes and their trends, this task is nontrivial for a number of reasons. For instance, our attempts to study $[(Ph_3P)_3Rh(Ph)]$ and $[(Ph_3P)_3Rh(F)]$ failed because of the second-order ^{31}P NMR spectrum displayed by the phenyl complex and insufficient solubility of the fluoride. The iodide and bromide ligands possess a greater steric bulk while exhibiting stronger trans influences compared with chloride. This may lead to change in mechanisms, for example, from pathway B to pathway A or competition of both, thus preventing the study from producing deconvolutable, mechanistically meaningful results. Furthermore, if pathway A is to some extent operational, both the larger steric bulk and the stronger trans influence of iodide compared with bromide and chloride should result in faster exchange for X = I. However, separating contributions from the electronic and steric effects to the overall exchange rate might be impossible. As for iridium, the inertness of its $[(Ph_3P)_3Ir(X)]$ analogues requires that the studies be carried out at higher temperatures, at which the complexes are unstable toward cyclometalation and other transformations. Although dealing with a limited number of models for the experimental studies, our work has led to important conclusions on mechanisms and factors that govern fluxionality of $[(R_3P)_3Rh(X)]$. Our results explain why certain $[(R_3P)_3Rh(X)]$ are highly fluxional (X = Alk,[8,9,13,15]

(64) Most recently, after our work was already completed, a paper appeared describing a computational study of PR_3 dissociation from $[(R_3P)_3Rh(Cl)]$ (R = H, Ph), albeit without denoting which phosphine is lost. See: Dachs, A.; Osuna, S.; Roglans, A.; Solà, M. *Organometallics* **2010**, *29*, 562.

Ar,[8,9,13,14] H,[11] CF_3[15,16]), displaying averaged or broad signals in their ^{31}P NMR spectra, whereas numerous others are less fluxional or rigid on the NMR time scale under similar conditions (X = F,[14,17] Cl,[2,10,12] Br,[65] CN,[20] OR,[18] NR_2,[19] NCS,[20] NCO,[20] N_3,[20] RCOO[20,66]).

Experimental Section

All chemicals were purchased from Aldrich and SynQuest chemical companies. The solvents were thoroughly dried using standard techniques and stored over freshly calcined molecular sieves (4 Å) in a glovebox. THF-d_8 was vacuum-transferred from Na/OCPh$_2$ and stored over 4 Å molecular sieves in a glovebox. Complexes [(Ph$_3$P)$_3$Rh(F)],[14,17] [(Ph$_3$P)$_3$Rh(Cl)],[67] [(Ph$_3$P)$_3$Rh(CH$_3$)],[8] [(Ph$_3$P)$_3$Rh(Ph)],[8] [(Ph$_3$P)$_3$Rh(H)],[68] and [(Ph$_3$P)$_3$Ir(Cl)][69] were synthesized by the literature procedures. The paramagnetic impurity-free (ESR) Wilkinson's catalyst was prepared as a crystalline precipitate on stirring of [(COD)$_2$Rh$_2$(μ-Cl)$_2$] with a 10-fold excess of PPh$_3$ in ether at 30 °C for 3 days.[70] All manipulations were performed under nitrogen in a glovebox. Routine NMR spectra were obtained with a Bruker Avance DRX400 spectrometer operating at 400 MHz. A Bruker-CCD instrument was used for single-crystal X-ray diffraction studies. A summary of the crystallographic data is presented in Table 10. Microanalyses were performed by Micro-Analysis, Inc., Wilmington, Delaware (in air), and Schwarzkopf Microanalytical Laboratory, Inc., Woodside, New York (under N_2).

Reaction of [(Ph$_3$P)$_3$RhF] with CF_3SiMe_3. Isolation and characterization of *trans*-[(Ph$_3$P)$_2$Rh(CF$_2$)(F)]. (A) To a mixture of [(Ph$_3$P)$_3$Rh(F)] (0.43 g; 0.47 mmol) in benzene (5 mL) was added, at agitation, CF_3SiMe_3 (78 μL; ca. 10% excess), and the mixture was vigorously stirred for 2 h 40 min until all solids had dissolved and then for additional 50 min. Hexanes (5 mL) was added in small portions until the dark orange-red solution turned cloudy and well-shaped crystals began to grow. After 1 h, more hexanes (5 mL) was added. After 2 h at room temperature, the crystals were separated, washed with hexanes (3 mL), and quickly dried with a flow of N_2. The product was recrystallized by dissolving in THF (ca. 5 mL) and adding hexanes (10 mL). After 1 h at −25 °C, the orange crystals were separated, washed with hexanes (3 × 1 mL), and dried under vacuum. The yield was 0.28 g (85% if calculated on [(Ph$_3$P)$_2$Rh(CF$_2$)(F)]). One crystal was analyzed by single-crystal X-ray diffraction to determine its structure as *trans*-[(Ph$_3$P)$_2$Rh(CF$_2$)(F)]. (B) To a mixture of [(Ph$_3$P)$_3$RhF] (0.30 g; 0.33 mmol) in benzene (4 mL) was added, at agitation, CF_3SiMe_3 (50 mg; 0.35 mmol), and the mixture was vigorously stirred for 2 h to give a solid-free dark red solution. Hexanes (4 mL) was added. After 1 day, the red crystals that formed were separated, washed with hexanes, and dried. The yield was 0.16 g (70% if calculated on [(Ph$_3$P)$_2$Rh(CF$_2$)(F)]). The product was identical to the material obtained in experiment A. (C) Experiment A was repeated. One crystal from the crop obtained upon addition of hexanes to the reaction solution (prior to recrystallization from THF−hexanes) was analyzed by single-crystal X-ray diffraction to determine its structure as *trans*-[(Ph$_3$P)$_2$Rh(CF$_2$)(F)]. This was a different polymorph with the two fluorine atoms on the carbene ligand disordered.[15] Anal. Calcd. for $C_{37}H_{30}F_3P_2Rh$, %: C, 63.8; H, 4.3. Found for A (under N_2), %: C, 64.4; H, 4.8; C, 64.1; H, 4.7. Found for B (under N_2), %: C, 64.4; H, 4.5; C, 64.3; H, 4.5. Found for A (in air), %: C, 65.2; H, 4.6; C, 65.0; H, 4.6. Found for B (in air), %: C, 65.3; H, 4.7; C, 65.1; H, 4.7.

The higher C values obtained from the combustion analysis in air are consistent with hydrolysis of the CF_2 ligand to carbonyl to produce *trans*-[(Ph$_3$P)$_2$Rh(CO)(F)], a known complex.[15,23,71]

Preparation of [(Ph$_3$P)$_3$Rh(CF$_3$)] (3). A mixture of [(Ph$_3$P)$_3$Rh(F)] (0.30 g; 0.33 mmol), benzene (4 mL), and CF_3SiMe_3 (50 mg, 0.35 mmol) was stirred for 2 h to give a solid-free deep red solution. Triphenylphosphine (0.50 g, 1.9 mmol) was added, and after complete dissolution the mixture was treated with hexanes (ca. 5 mL). After two days, red cubic crystals precipitated. The crystals were separated, washed with hexanes, and dried. The yield of **3** was 0.265 g (84%). One of the crystals was analyzed by single-crystal X-ray diffraction. NMR (C_6D_6, in the presence of 6 equiv of PPh$_3$, 20 °C), δ: ^{19}F −2.4 (dq, J_{F-P} = 32 Hz, J_{F-Rh} = 11.5 Hz); ^{31}P 29.4 (dq, J_{P-F} = 32 Hz, J_{P-Rh} = 158 Hz). Anal. Calcd. for $C_{55}H_{45}F_3P_3Rh$, %: C, 68.9; H, 4.7. Found (under N_2), %: C, 68.5; H, 4.8. Found (in air), %: C, 68.8; H, 4.9.

When precipitation of **3** was done under not rigorously anhydrous conditions a small quantity of a second type of crystal was observed.

Table 10. A Summary of Crystallographic Data for the Orange and Red Forms of **2**

	[(Ph$_3$P)$_3$Ir(Cl)] (**2**), orange	[(Ph$_3$P)$_3$Ir(Cl)] (**2**), red
empirical formula	$C_{54}H_{45}ClIrP_3$	$C_{54}H_{45}ClIrP_3$
FW	1014.46	1014.46
cryst color, form	gold, cube	red, irreg. block
cryst syst	orthorhombic	orthorhombic
space group	$Pna2_1$	$Pna2_1$
a (Å)	19.358(3)	32.705(9)
b (Å)	12.646(2)	12.187(3)
c (Å)	18.038(3)	10.985(3)
V (Å^3)	4416(1)	4379(2)
Z	4	4
density (g/cm^3)	1.526	1.539
abs. μ (mm^{-1})	3.230	3.257
F(000)	2032	2032
cryst size (mm^3)	0.08 × 0.08 × 0.08	0.05 × 0.08 × 0.18
temp (°C)	−100	−100
scan mode	ω	ω
detector	Bruker-CCD	Bruker-CCD
θ_{max} (deg)	26.38	28.92
no. obsd reflns	39468	81944
no. unique reflns	8987	11452
R_{merge}	0.12	0.08
no. params	532	532
S^a	0.96	1.01
R indices [$I > 2\sigma(I)$]^b	wR2 = 0.067 R1 = 0.044	wR2 = 0.060 R1 = 0.030
R indices (all data)^b	wR2 = 0.081 R1 = 0.090	wR2 = 0.064 R1 = 0.043
max diff peak, hole (e/Å^3)	0.84, −0.83	1.67, −0.73

^{a} GOF = $S = \{\sum[w(F_o^2 - F_c^2)^2]/(n-p)\}^{1/2}$, where n is the number of reflections and p is the total number of refined parameters. ^{b} R1 = $\sum||F_o| - |F_c||/\sum|F_o|$; wR2 = $\{\sum[w(F_o^2 - F_c^2)^2]/\sum[w(F_o^2)^2]\}^{1/2}$ (sometimes denoted as R_w2).

(65) (a) In the original 1970 article,[65b] it was reported that for [(Ph$_3$P)$_3$Rh(Br)] and [(Ph$_3$P)$_3$Rh(I)], well-resolved ^{31}P NMR multiplets could be observed only below 10 and −10 °C, correspondingly. The samples were prepared by dissolving the complexes in dichloromethane in air, followed by bubbling N_2 through the solution prior to NMR measurements. More recently, an A_2BX ^{31}P NMR spectrum was recorded at −10 °C for a sample prepared by dissolving [(Ph$_3$P)$_3$Rh(I)] in CD_2Cl_2 under N_2, using a glovebox or a Schlenk line.[65c] We have observed a well-resolved A_2BX pattern in the ^{31}P NMR spectrum of [(Ph$_3$P)$_3$Rh(Br)] in THF at 20 °C for a sample prepared under rigorously dry, O_2-free conditions in a glovebox. (b) Brown, T. H.; Green, P. J. *J. Am. Chem. Soc.* **1970**, *92*, 2359. (c) Colebrooke, S. A.; Duckett, S. B.; Lohman, J. A. B.; Eisenberg, R. *Chem.—Eur. J.* **2004**, *10*, 2459.

(66) Carlton, L. *Magn. Reson. Chem.* **1997**, *35*, 153.

(67) Osborn, J. A.; Wilkinson, G. *Inorg. Synth.* **1990**, *28*, 77.

(68) Esteruelas, M. A.; Herrero, J.; Oliván, M. *Organometallics* **2004**, *23*, 3891.

(69) Bennett, M. A.; Latten, J. L. *Inorg. Synth.* **1989**, *26*, 200.

(70) (a) The method is similar to the one described in: Ogle, C. A.; Masterman, T. C.; Hubbard, J. L. *J. Chem. Soc., Chem. Commun.* **1990**, 1733. (b) See also: Dunbar, K. R.; Haefner, S. C. *Inorg. Chem.* **1992**, *31*, 3676.

(71) (a) Vaska, L. *Inorg. Synth.* **1974**, *15*, 64. (b) Wierzbicki, A.; Salter, E. A.; Hoffman, N. W.; Stevens, E. D.; Do, L. V.; VanLoock, M. S.; Madura, J. D. *J. Phys. Chem.* **1996**, *100*, 11250.

These crystals were identified as *trans*-[$(Ph_3P)_2Rh(CO)(F)$], which is believed to be formed upon facile hydrolysis of the difluorocarbene ligand in *trans*-[$(Ph_3P)_2Rh(CF_2)(F)$] existing in equilibrium with **3** in solution (see above).

Preparation of Samples of [$(Ph_3P)_3M(X)$] (M = Rh, Ir) for VT NMR Studies. A 3:2 mixture of THF-h_8 and THF-d_8 was used for all experiments. A solution of **3** for the NMR study was prepared by dissolving preisolated *trans*-[$(Ph_3P)_2Rh(CF_2)(F)$] (20 mg from experiment A, see above) and PPh_3 (115 mg; 15-fold excess) in 0.7 mL of the solvent. As originally reported by Keim,[8] both complexes [$(Ph_3P)_3Rh(X)$] (X = Me, Ph) undergo facile cyclometalation. It was found that while the cyclometalation reaction can be efficiently suppressed for the Ph complex by addition of 2−4 equiv of PPh_3, the Me analog cyclometalated at room temperature even in the presence of 15 equiv of extra phosphine. The NMR samples were prepared by dissolving the complexes in solutions of PPh_3 (6 equiv for Rh−Ph; 15 equiv for Rh−Me). In order to avoid the cyclometalation reaction of the methyl complex, the freshly prepared solution in a sealed standard 5 mm NMR tube was immediately placed in the precooled probe of the spectrometer. At the low temperatures used for the study (−10 °C and below), no cyclometalation for the thus prepared sample of [$(Ph_3P)_3Rh(Me)$] was observed. The sample of [$(Ph_3P)_3Rh(Ph)$] containing 6 equiv of PPh_3 was stable toward cyclometalation in the entire range of temperatures up to 40 °C. The hydride [$(Ph_3P)_3Rh(H)$] was studied in the absence of extra PPh_3 to avoid the facile formation of [$(Ph_3P)_4Rh(H)$]. All samples of **1** and **2** were saturated solutions containing ca. 2−8 equiv of extra PPh_3 to avoid the formation of [$(Ph_3P)_4Rh_2(\mu\text{-}Cl)_2$] and allow for the intermolecular exchange studies.

Kinetic Measurements and VT NMR Studies. Magnetization transfer experiments were performed on a Varian Unity Inova spectrometer operating at 400 MHz for ^1H and 161.9 MHz for ^{31}P. The high-power ^{31}P 90° observe pulse was 9.5 μs, while the selective 180° inversion pulse (IBURP2) was optimized to give a selective pulse of minimal duration by using the Varian Pbox routine. The delay time between the selective inversion pulse and the 90° readout pulse was typically arrayed from 1 ms to 10 s in order to map out the time dependence of the intensity changes. The general protocol for the magnetization transfer experiments was to selectively invert one site and to monitor the return to equilibrium of the inverted site as well as the transient changes in intensity of the exchange partners. The experiment was then repeated by selectively inverting the other sites in turn. The exchange matrix was formulated in the standard fashion,[72] and rate constants were obtained by iterative adjustment of the equilibrium and initial magnetization integrated intensities, the T_1's, and the rate constants to provide the least-squares best fit to the experimental data along with standard deviations for the parameter estimates.[73]

Computational Studies. Computations were run with Gaussian 03[74] with geometry optimizations using the BP86 functional.[75] Rh, P, and Cl centers were described with the Stuttgart RECPs and associated basis sets,[76] with added d-orbital polarization on P and Cl (ζ = 0.387 and 0.640, respectively);[77] 6-31G** basis sets were used for all other atoms.[78] All stationary points were fully characterized via analytical frequency calculations as either minima (all positive eigenvalues) or transition states (one imaginary eigenvalue), and IRC calculations and subsequent geometry optimizations were used to confirm the minima linked by each transition state. The same basis set/pseudopotential choices as above were employed for the single-point energy calculations at the MP2 level and selected calculations with the M06[39] functional, the latter being run with Gaussian 09.[79]

Acknowledgment. This is DuPont CRD Contribution No. 8932. We thank Prof. John M. Brown of the University of Oxford for valuable comments. Dr. Vladimir I. Bakhmutov of Texas A&M University is gratefully acknowledged for numerous helpful discussions, and we thank Prof. Jeremy Harvey (University of Bristol) for use of the MECP location program. A reviewer is also thanked for helpful comments regarding the role of spin-crossover processes on the overall rate of intramolecular exchange in [$(Ph_3P)_3Rh(Cl)$]. J.G. thanks Heriot-Watt University and the EPSRC for support.

Supporting Information Available: Complete refs 74 and 79 and full details of all computed structures and energies (PDF) and X-ray analysis data for the red and orange forms of **2** (CIF). This material is available free of charge via the Internet at http://pubs.acs.org.

JA1039693

(72) Binsch, G. In *Dynamic Nuclear Magnetic Resonance Spectrsocopy*; Jackman, L. M., Cotton, F. A., Eds.; Academic Press: New York, 1975; pp 51−52.

(73) Roe, D. C. *Organometallics* **1987**, *6*, 942.

(74) Frisch, M. J.; et al. *Gaussian 03*, revision C.02; Gaussian Inc.: Wallingford, CT, 2004.

(75) (a) Becke, A. D. *J. Chem. Phys.* **1993**, *98*, 1372. (b) Becke, A. D. *J. Chem. Phys.* **1993**, *98*, 5648. (c) Perdew, J. P. *Phys. Rev. B* **1986**, *33*, 8822.

(76) Andrae, D.; Haussermann, U.; Dolg, M.; Stoll, H.; Preuss, H. *Theor. Chim. Acta* **1990**, *77*, 123.

(77) Höllwarth, A.; Böhme, M.; Dapprich, S.; Ehlers, A. W.; Gobbi, A.; Jonas, V.; Köhler, K. F.; Stegmann, R.; Veldkamp, A.; Frenking, G. *Chem. Phys. Lett.* **1993**, *208*, 237.

(78) (a) Hehre, W. J.; Ditchfield, R.; Pople, J. A. *J. Chem. Phys.* **1972**, *56*, 2257. (b) Hariharan, P. C.; Pople, J. A. *Theor. Chim. Acta* **1973**, *28*, 213.

(79) Frisch, M. J.; et al. *Gaussian 09*, revision A.02; Gaussian Inc.: Wallingford, CT, 2009.